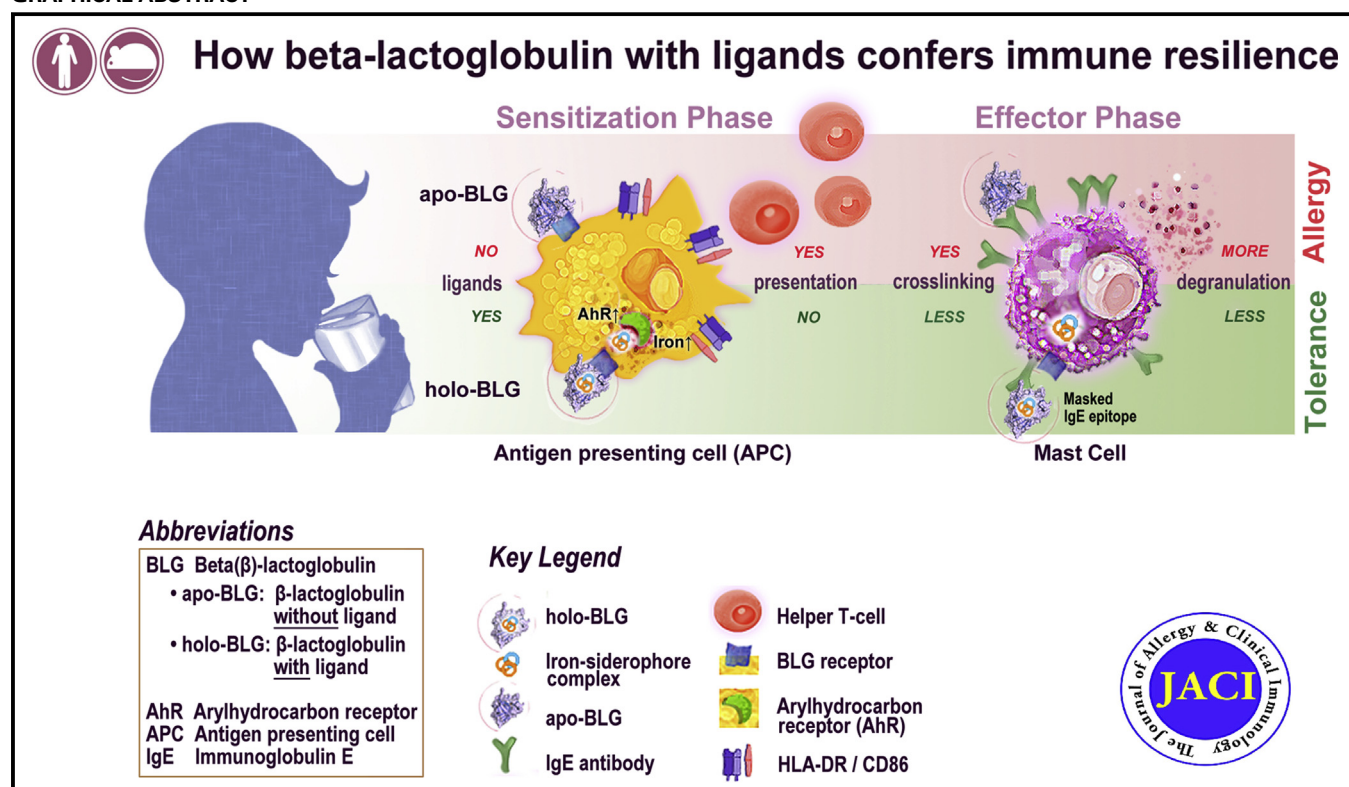## Mechanisms of allergy/immunology

Cow's milk protein β-lactoglobulin confers resilience against allergy by targeting complexed iron into immune cells

Check for updates

Franziska Roth-Walter, PhD,[a,b] Sheriene Moussa Afify, MD,[a,c] Luis F. Pacios, PhD,[d] Bart R. Blokhuis, Ing,[e] Frank Redegeld, PhD,[e] Andreas Regner, MSc,[a] Lisa-Marie Petje, BSc,[a] Alessandro Fiocchi, MD,[f] Eva Untersmayr, MD,[b] Zdenek Dvorak, PhD,[g] Karin Hufnagl, PhD,[a,b] Isabella Pali-Schöll, PhD,[a,b] and Erika Jensen-Jarolim, MD[a,b] *Vienna, Austria; Menoufia, Egypt; Madrid, Spain; Utrecht, The Netherlands; Rome, Italy; and Olomouc, Czech Republic*

GRAPHICAL ABSTRACT

https://doi.org/10.1016/j.jaci.2020.05.023

Background: Beta-lactoglobulin (BLG) is a bovine lipocalin in milk with an innate defense function. The circumstances under which BLG is associated with tolerance of or allergy to milk are not understood.

Objective: Our aims were to assess the capacity of ligand-free apoBLG versus loaded BLG (holoBLG) to protect mice against allergy by using an iron-quercetin complex as an exemplary ligand and to study the molecular mechanisms of this protection.

Methods: Binding of iron-quercetin to BLG was modeled and confirmed by spectroscopy and docking calculations. Serum IgE binding to apoBLG and holoBLG in children allergic to milk and children tolerant of milk was assessed. Mice were intranasally treated with apoBLG versus holoBLG and analyzed immunologically after systemic challenge. Aryl hydrocarbon receptor (AhR) activation was evaluated with reporter cells and Cyp1A1 expression. Treated human PBMCs and human mast cells were assessed by fluorescence-activated cell sorting and degranulation, respectively.

Results: Modeling predicted masking of major IgE and T-cell epitopes of BLG by ligand binding. In line with this modeling, IgE binding in children allergic to milk was reduced toward holoBLG, which also impaired degranulation of mast cells. In mice, only treatments with holoBLG prevented allergic sensitization and anaphylaxis, while sustaining regulatory T cells. BLG facilitated quercetin-dependent AhR activation and, downstream of AhR, lung Cyp1A1 expression. HoloBLG shuttled iron into monocytic cells and impaired their antigen presentation.

Conclusion: The cargo of holoBLG is decisive in preventing allergy *in vivo*. BLG without cargo acted as an allergen *in vivo* and further primed human mast cells for degranulation in an antigen-independent fashion. Our data provide a mechanistic explanation why the same proteins can act either as tolerogens or as allergens. (J Allergy Clin Immunol 2021;147:321-34.)

Key words: Allergen, allergy, β-lactoglobulin, BLG, Bos d 5, cow's milk, iron, ligand, lipocalin, milk, quercetin, tolerance

The prevalence of allergies is rising in the westernized world, which has been partly attributed to living in a "too-clean" environment and which is also affected by lifestyle factors.[1] Numerous studies have shown that exposure to farms,[2] as well as consumption of unprocessed farm milk during the first years of life, protects against atopic eczema, hay fever, and asthma.[3] In the case of farm milk, the reduced allergy risk[4-6] is particularly associated with the whey protein content: the more native, undestroyed whey proteins are present, the more the milk is considered protective.[7,8] Notably, roughly half of the whey proteins are constituted by β-lactoglobulin (BLG). It seems a paradox that at the same time, BLG is considered a major milk allergen to which the majority of individuals allergic to milk are sensitized.[9,10] Importantly, despite comparable milk consumption, only certain individuals will become allergic to milk, strongly suggesting that cofactors such as their ligands might be decisive in the sensitization process.

BLG belongs to the lipocalin (LCN) protein family, to which nearly all major allergens from mammals belong, and which show a highly conserved fold despite having very low amino acid sequence homology.[11]

In humans, BLG is found to be immune cell–associated,[12] implying that transport of BLG occurs via the lymphatics rather than via the blood vessels. Cellular BLG uptake in humans occurs via specific receptors[13-16] that were originally tailored for

Abbreviations used
AhR: Aryl hydrocarbon receptor
β-hex: β-hexosaminidase
BLG: β-Lactoglobulin
FeQ2: Iron–quercetin 2
LCN: Lipocalin
SCF: Stem cell factor
TBS: Tris-buffered saline
Treg: Regulatory T
UV-VIS: Ultraviolet-visible spectroscopy

endogenous human LCN proteins such as LCN2[17,18] or LCN1.[19] We have previously demonstrated the high molecular similarity of human LCN2 and BLG,[20] implying receptor sharing.

Similar to LCN2[21] and LCN1,[22] BLG can bind to catechol-type siderophores,[18,23] which are small molecules with a strong affinity to ferric iron, thereby withholding iron and impeding bacterial growth.[24]

Other BLG ligands that have been described include fatty acids,[25] retinoic acid,[26] and polyphenols/flavonoids,[27] such as quercetin[28] and catechin,[25,27,29,30] which also have a very strong affinity to iron at physiologic pH.[31,32] The reported complex stability constant log ß values of these polyphenols range from 44 to 47,[31] which is comparable to the iron-sequestering abilities of siderophores of bacterial origin.[20,33,34]

In the present study, quercetin was chosen as an exemplary ligand for BLG because (1) quercetin can complex iron with a high affinity[23,31,35] similar to that of bacterial siderophores, thus better mimicking the natural innate function of BLG compared with fatty acids only; (2) it is a ligand reported to bind to BLG[36,37] and other allergens[38-40]; (3) it is present in milk, as it is transferred via the cow's plant chow to the milk[41] and consequently may represent a natural interaction partner of BLG in milk; and (4) quercetin *per se* has known anti-inflammatory properties.[42]

As siderophore binding of human LCN2[17,18,43-46] is decisive in activating or suppressing our immune system,[23] we sought to investigate whether BLG, which already exploits LCN pathways, may similarly modulate our immune response by ligand binding.

In a previous publication, we have already demonstrated that the loaded holo form of BLG is immunosuppressive and only the ligand-free apo form is able to evoke an immune response *in vitro*.[23] Consequently, here we address the *in vivo* relevance and mechanistic explanations for the observed "immune shutdown."

We show that the immunosuppressive tolerogenic properties of BLG are closely linked with shuttling the FeQ2 complex to innate cells. Ligand binding masked a major B-cell epitope on BLG and affected specific antigen recognition; in addition, both iron and quercetin *per se* promoted a resilience to immune activation by impairing antigen presentation via transport of iron and activation of the aryl hydrocarbon receptor pathway. The results identify the transport of environmental or nutritional ligands by BLG to immune cells as being pivotal in the induction of immune tolerance and underscore their potential in preventing and treating allergic disorders.

METHODS
Ethical approval

Volunteers donated blood after providing written informed consent. The study was approved by the ethics committee (approval no. 1972/2017) of the

Medical University of Vienna and conducted in accordance with the principles of the Helsinki Declaration of 1975. Sera of patients with milk allergy (20 patients who tested positive and 20 patients who tested negative to oral cow's milk allergen challenge) were retrospectively collected in accordance with the principles of the Helsinki Declaration of 1975 and under approval of the ethical committee of the Bambino Gesù Pediatric Hospital, Rome, Italy; individual informed consent from all donors was collected by Dr Alessandro Fiocchi of Children's Hospital Bambino Gesú, Rome, Italy. Open food challenges, as described in the American Academy of Allergy, Asthma & Immunology/Europrevall protocol,[47] were performed to confirm milk allergy. Children who had no symptoms with cumulative administration of the entire milk dose corresponding to 144 mL were considered negative.

Animals

Female BALB/c mice, 5 to 7 weeks of age, were obtained from Charles River Laboratories (Bad Königshofen, Germany), kept under conventional housing, and treated according to European Union rules of animal care with the permission of the Austrian Ministry of Sciences (BMWF-66.009/0133-WF/V/3b/2016).

Structural and docking analysis

BLG structure was taken from the complex with retinoic acid (Protein Data Bank entry 1GX9).[48] The geometries of quercetin were obtained following energy minimization with the MM2 force field of initial structures drawn by using the ChemBioDraw/ChemBio3D Ultra 12.0 software package. Docking input files for protein and ligands were prepared with AutoDockTools.[49] A grid box of 22 Å × 22 Å × 22 Å with origin at a point corresponding to the C6 atom in the retinoic acid molecule in the 1GX9 structure was used for docking calculations, which were performed with AutoDock Vina.[50] The docking geometry with the lowest affinity energy was selected. Estimates of dissociation equilibrium constants were then calculated for the protein-ligand complexes by assuming the following: $E_{aff} \sim \Delta G$ with $K_d = \exp(-\Delta G/RT)$ at T = 298.15, where E_{aff} is the lowest affinity energy and K_d is the dissociation equilibrium constant.

Protein structural diagrams were prepared by the UCSF Chimera and Pymol (PyMOL Molecular Graphics System, version 1.8 Schrödinger, LLC, 2015[51,52]). Surface area, solvation energy, and solvation effect calculations were performed by using the PISA module of the CCP4 package.[53] Ligand Explorer was used to analyze the ligand-protein interaction and measure distances, which were further validated by the NCONT module of CCP4.[54]

Spectral analysis

For spectral analysis, 0.9% NaCl (for Fig 1, *C*) or deionized water (Fig 1, *D*) was used as a buffer to minimize iron contamination from the air. The pH was kept constant at 7 by addition of NaOH. Fluorescence was measured by exiting samples at 450 nm and measuring emission in 20-nm steps starting from 480 and extending to 800 nm by using a Tecan InfiniteM200 PRO reader (Männedorf, Switzerland). Optical density was measured at a constant concentration of 100 μM quercetin or 50 μM iron, BLG or deferoxamine, and combinations thereof. All measurements were repeated at least 3 times with similar results.

Generation of apoBLG and holoBLG

Commercially available bovine BLG (L0130, Sigma, Darmstadt, Germany) was dissolved in deionized water (20 mg/mL) and dialyzed 3 times against 10 μM deferoxamine mesylate salt. Further dialyzation against deionized water was performed (apo–*Bos domesticus* 5). HoloBLG was generated by forming iron–quercetin 2 (FeQ2) complexes with quercetin (Sigma 1592409) and iron (iron standard AAS, Sigma 16596) at a ratio 2:1 and adjusting the pH to 7.2 with 10 mM NaOH and adding apoBLG to a final concentration of 1 μM BLG, 2 μM quercetin, and 1 μM iron.

Allergic sensitization and challenge of mice

Sample size for the mouse experiments were based on the literature. No randomization was performed. We estimated natural exposure to BLG for a 20-kg child consuming daily a 200-mL glass cow's milk roughly equivalent to 1 g of BLG, which corresponds to consumption of 1 mg of BLG by a 20-g mouse. In our settings, we estimated a 100-fold lower local mucosal concentration by applying 10 μg of BLG (5 μg per nostril) to the respected groups. As such, the mice were split into groups of 5 to 7 animals and treated 6 times on 2 consecutive days intranasally with 10 μL per mouse (5 μL per nostril) containing (1) 10 μg of apoBLG (0.5 nM) and 0.3 μg of deferoxamine (~0.5 nM); (2) holoBLG (0.5 nM BLG with 0.5 nM iron [28 ng]) and 1 nM quercetin 2 (338 ng); (3) FeQ2 complex (0.5 nM iron [28 ng] and quercetin 2 (338 ng); or (4) deferoxamine. One week later, the mice were intranasally challenged with 20 μg of BLG on 2 consecutive days and intraperitoneally challenged 24 hours later with 50 μg of BLG in 0.9% NaCl. Four mice from different groups were challenged at each cycle. The investigator who challenged and scored the animals was blinded to the group to which the mice belonged. The animals were scored as previously described,[12] giving 0 points for no symptoms; 1 point for scratching and rubbing around the nose and head; 2 points for puffiness around the eyes and mouth, diarrhea, pilar erecti, reduced activity, and/or decreased activity with increased respiratory rate; 3 points for wheezing, labored respiration, and cyanosis around the mouth and the tail; and 4 points for no activity after prodding or tremor and convulsion. Body temperature and movements were monitored for 20 minutes by using the Imaging system (Biomedical International R+D GmbH, Vienna, Austria).[55] After the mice had been humanely killed with CO_2, blood was collected by cardiac puncture and sera were stored at −80°C until further processing. Spleens and lungs were collected. Lungs were perfused with 0.9% NaCl, before fixation in 3.7% neutral paraformaldehyde and paraffin-embedding. For histologic analysis, 5-μm-thick sections were taken. Results of 3 separate independent experiments were compared.

Measurement of mouse serum antigen-specific antibodies by ELISA

BLG-specific IgG1, IgA, IgG2a, and IgE levels were measured by ELISA. Briefly, BLG (1 μg per well) or serial dilutions of mouse IgG1, IgG2a, IgE, and IgA standards (highest concentration for IgG1, IgG2a, and IgA, 1000 ng/L; for IgE standard, 100 ng/mL) were coated, blocked with 1% BSA in PBS, and incubated with diluted sera (1:100 for IgG1, IgG2a, and IgA and 1:15 for IgE) overnight at 4°C. Specific antibodies were detected with the rat anti-mouse mAbs IgG1 (clone A85-1), IgG2a (clone R19-15), IgA (clone c10-1), or IgE (clone R35-72), followed by polyclonal peroxidase-labeled goat anti-rat IgG (GE Healthcare, Vienna, Austria). Tetramethylbenzidine (eBioscience, San Diego, Calif) was used as the substrate and 1.8 M sulfuric acid was used as the stop solution, followed by optical density measurement at 450 nm.

Measurement of BLG-specific antibodies of milk sensitized children by ELISA

Quantities of 5 μg/mL of apoBLG, BLG with an equimolar concentration of deferoxamine, or holoBLG diluted in 0.89% NaCl were coated (100 μL per well) overnight at 4°C. After 2 hours of blocking at room temperature with 0.89% NaCl (200 μL per well) containing plus 0.05% Tween 20 and 0.05% albiomin (20%, 200g/L Biotest, CSL Behring, Kankakee, Ill), the wells were incubated with 100 μL of human serum diluted 1:10 in 0.89% NaCl containing 0.05% Tween-20 overnight at 4°C. Detection was performed by using horseradish peroxidase–conjugated goat anti-human IgE antibody (Invitrogen A18793) diluted at 1:4000 in 0.89% NaCl containing 0.05% Tween-20, with use of tetramethylbenzidine (eBioscience) as a substrate and 1.8 M sulfuric acid to stop color development. The optical density was measured at 405 nm by using an Infinite M200Pro microplate reader (Tecan, Austria). Between the steps rigorous washing was performed with 0.89% NaCl containing 0.05% Tween-20.

In vitro cytokine response of stimulated splenocytes and human PBMCs

Isolated splenocytes of individual mice were plated at a density of 5×10^6 cells/mL and cultured with 5 and 25 μg/mL of BLG or 5 μg/mL of holoBLG,
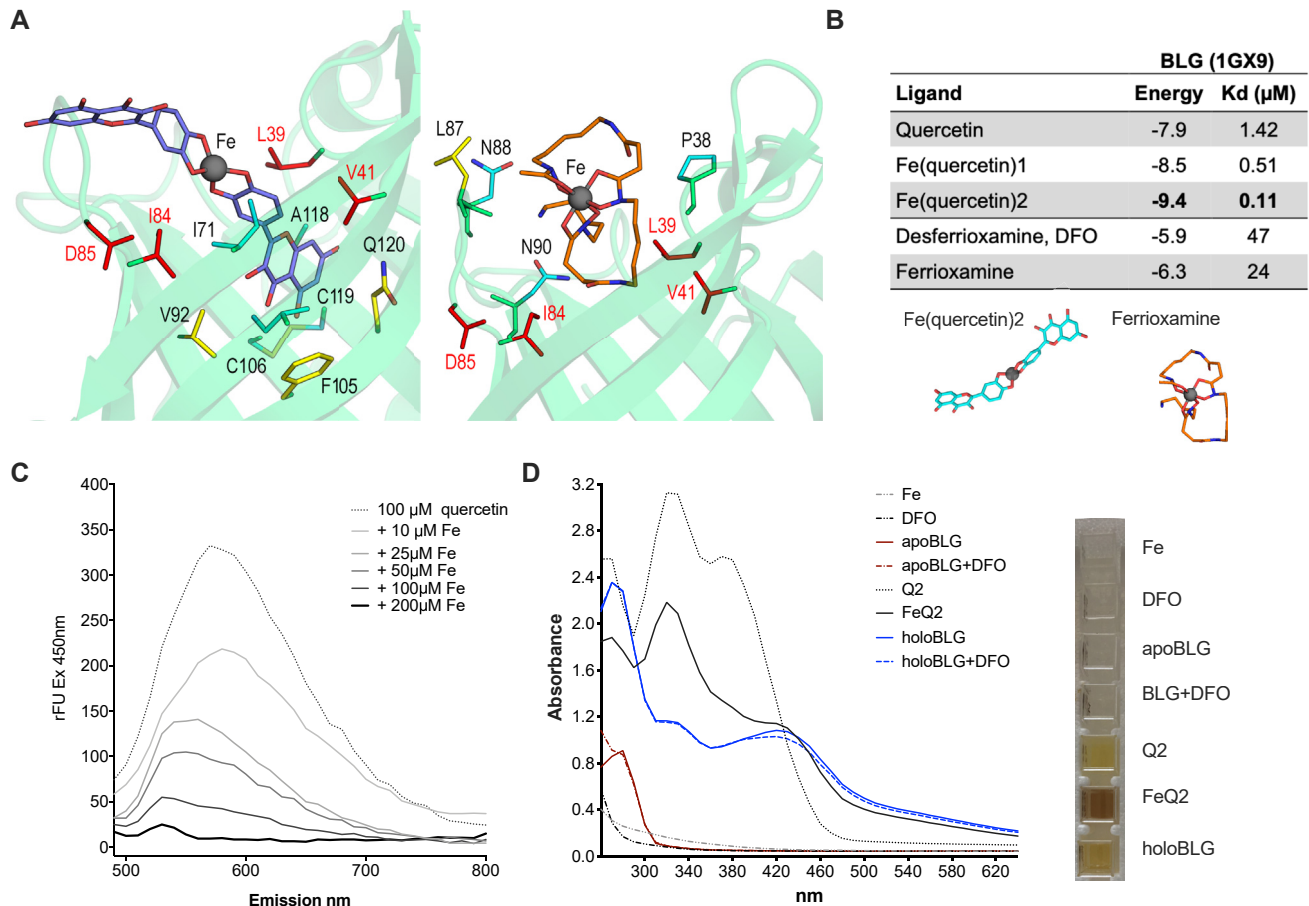
FIG 1. FeQ2 complex formation and binding to BLG. **A,** Model of BLG incorporating FeQ2 or ferrioxamine complexes. **B,** Calculated affinities of quercetin as described by Roth-Walter et al[23] and desferrioxamine in the presence and absence of iron to BLG by AutoDock VINA. **C,** Fluorescence quenching of quercetin following addition of iron. **D,** Optical spectra and color change of 100 μM quercetin and 50 μM desferrioxamine, iron, BLG, and combinations thereof at pH 7.3.

2.5 μg/mL of concanavalin A (Sigma), or medium alone for 72 hours at 37°C and 5% CO_2.

Blood cells were lysed for 10 minutes with red blood cell lysis buffer (eBioscience) and washed before the peripheral blood cells were incubated with BLG (10 μM), iron, quercetin, and combinations thereof in media containing neither phenol red nor FCS for 18 hours.[35] Secreted mouse and human cytokines were measured with the corresponding commercial ELISAs for human or mouse IL-10, IL-13, and IFN-γ (Invitrogen/eBioscience) according to the manufacturer's instructions.

AZ-AHR cells

Cells of the AZ-AHR cell line are human hepatoma HepG2 cells transfected with pGL-4.27-DRE construct containing several arylhydrocarbon receptor (AhR) binding sites upstream of luciferase reporter gene, as previously described.[56,57] AZ-AHR cells were cultured in Dulbecco modified Eagle medium (Gibco, Waltham, Mass) without phenol red that was supplemented with 10% of FCS, 100 U/mL of streptomycin, 100 μg/mL of penicillin, 4 mM L-glutamine, 1% nonessential amino acids, and 1 mM sodium pyruvate. At biweekly intervals, 0.2 mg/mL of hygromycin B (Sigma) was added to the culture. Cells were maintained at 37°C and 5% CO_2 in a humidified incubator. During stimulation experiments, the same medium as already described, but without 10% FCS, was used. Cells were routinely tested for mycoplasma contamination.

AZ-AHR cell reporter assay

AZ-AHR cells were incubated at 37°C and 5% CO_2 on 96-well plates at a density of 2×10^4 cells per well for 18 hours. Subsequently, cells were stimulated for 18 hours in triplets with 90 μM quercetin alone or in complex with iron and increasing concentrations of BLG (5 μM and 10 μM). Compounds were first incubated together for 15 minutes, and the pH was adjusted to 7 before addition of BLG. The positive control was treated with 20 nM indirubin. Cells were washed once with 0.89% NaCl and lysis buffer was added. After a single freeze-thaw cycle, the lysates (20 μL per well) were transferred to a black 96-well flat-bottom plate (Thermo Scientific, Waltham, Mass) and the bioluminescent reactions were started with addition of 100 μL per well of luciferase assay reagent (Promega, Madison, Wis). Chemiluminescence was measured (10 seconds per well) by using a spectrophotometer Tecan InfiniteM200 PRO.

Flow cytometric analyses

PBMCs were isolated by Ficoll-Paque (GE Healthcare)[23,35,57] and washed with 0,9% NaCl before the PBMCs were incubated with BLG (10 μM), iron, quercetin, and combinations thereof in media containing neither phenol red nor FCS for 18 hours.[35] We measured only a single time point because of the technical limitations that we encounter when working with iron. All media and buffers had to be iron-free and devoid of potential interaction partners (eg, phenol red) even though it is essential for cell survival. As such, the PBMCs had to be cultivated without any FCS, as longer time points would have overshadowed the "immediate" impact of iron.

Subsequently, cells were stained with combinations of calcein-AM (Thermo-Fisher), CD3-APC-Cy7 (eBioscience, clone SK7), CD14-APC-Cy7 (Biolegend, clone M5EZ), HLADR-PE (Biolegend, San Diego, Calif, clone L243PC), and CD86-PE-CY7 (Biolegend,clone IT2.2) for flow cytometric analysis.

For murine splenocytes, single-cell suspensions (0.5 million cells) were stained for $CD4^+Foxp3^+$ regulatory T (Treg) cells by using anti-FOXP3 PE (eBioscience, clone FJK-16s) and anti–CD4-FITC (eBioscience, clone RM4-5) antibodies, according to the manufacturer's instructions (eBioscience, catalog no. 88-8111). Doublets were excluded before gating to the lymphocytic cells and plotting to $CD4^+Foxp3^+$ cells. A second set of cells was stained for $CD71^+$ as a marker for proliferation by using anti-CD71 PE (eBioscience, clone R17217) and using calcein as a living marker. Here, doublets were first excluded before gating on the living cells as calcein positive and gating on the lymphocytic population on the FSC/SSC plot, followed by gating on the $CD71^+$ population. Cells were acquired by flow cytometry (BD Bioscience, Franklin Lakes, NJ, Canto II machine). Acquired cells were analyzed by using the FACSDiva software, version 6.0. Figure preparation for the PBMCs was conducted with cytoflow 1.0.

Immunohistochemical staining

Lung sections were stained for Cyp1A1. Briefly, unlabeled CYP1A1 (clone B-4, Santa Cruz Biotechnology, Dallas, Tex) was conjugated to alkaline phosphatase by using a commercial kit (Lightning-Link Alkaline Phosphatase Conjugation Kit, Innova Biosciences, Cambridge United Kingdom) according to the manufacturer's recommendation. After deparaffinization, heat-mediated antigen retrieval (30 minutes in 1 mM Tris-EDTA, pH9) and blocking with anti-mouse CD16/CD32 (1:100, in 2% FCS/Tris-buffered saline [TBS] for 30 minutes), slides were incubated overnight at 4°C with alkaline phosphatase–conjugated anti-mouse Cyp1A1 antibody (1:50 in TBS) before the addition of 5-bromo-4-chloro-3-indolyl phosphate–nitro blue tetrazolium as a substrate. Slides were counterstained with methyl green and mounted with resinous mounting medium (Sigma). Between each step, vigorous washing was performed with TBS. Images were acquired and manually quantified with a Zeiss (Oberkochen, Germany) Axio Imager Z1 microscope at ×20 magnification.

Human mast cell generation

$CD34^+$ derived human mast cells were generated from surplus autologous stem cell concentrates as previously described.[58] Briefly, frozen stem cell concentrates were rapidly thawed at 37°C under sterile conditions and poured into a large cell culture flask (Greiner, Kremsmünster, Austria). Next, 20% human serum albumin clinical solution (Sanquin, Amsterdam, The Netherlands), 6% hydroxyethyl starch clinical solution (Braun, Kronberg, Germany), and RPMI 1640 medium containing 10 U/mL of heparin (LEO Pharma, Ballerup, Denmark) were then added slowly and consecutively to the cell concentrate. Cells were then filtered through a cell dissociation sieve (Sigma) and incubated with DNAse (200 UI/mL, Roche, Basel, Switzerland) for 15 minutes. After washing, cells were resuspended in PBS containing 4% human serum albumin and then incubated with Fc-Block (Miltenyi, Auburn, Calif) for 15 minutes, $CD34^+$ positive selection cocktail (StemCell, Vancouver, Canada) for 15 minutes, and nanoparticles for 10 minutes. Subsequently, $CD34^+$ cells were sorted with an EasySep R Magnet (StemCell) according to the manufacturer's protocol. Finally, sorted cells were resuspended in serum-free expansion medium (StemCell) supplemented with human low-density lipoprotein (50 µg/mL, StemCell). On day 1, human recombinant IL-3 (100 ng/mL, Biolegend, San Diego, Calif), and stem cell factor (SCF) (100 ng/mL Miltenyi) were added. Every 3 to 4 days, IL-3 and SCF were added at a final concentration of 20 ng/mL At the end of the second week, mast cells were maintained under 20 ng/mL of SCF with the withdrawal of IL-3. After 4 weeks, the cells were cultured in Iscove modified Dulbecco medium and 0.5% BSA with human IL-6 (50 ng/mL, Peprotech, Rocky Hill, NJ) and 3% supernatant of Chinese hamster ovary transfectants secreting murine SCF (a gift from Dr P. Dubreuil, Marseille, France). The mature mast cells were identified by flow cytometry based on positive staining for CD117 (eBioscience) and FcεRIa (eBioscience, San Diego, Calif) using BD FACSCanto II (approximately 90%).

Human mast cell degranulation assay

The antigen-independent approach used was as follows: primary human mast cells ($0.8\ 10^6$/mL) were sensitized with 10% mouse hybridoma IgE supernatant (clone 26-82) overnight, washed with RPMI 1640 without phenol red that contained 1% FCS and 1 mM Glutamax, and counted, after which a 50-µL cell suspension (40 000 cells per well) was incubated for 2 hours without or with a 5, 50, 500, or 5000 nM BLG; holoBLG; Q2; and FeQ2 complex, before cross-linking with rat anti-mouse IgE (1 ug/mL, BD Pharmingen) for 60 minutes at 37°C. For β-hexosaminidase (β-hex) assay, cell-free supernatants were collected after 60 minutes and incubated with 200 µM 4-methylumbelliferyl-β-d- glucosaminide in 100mM citric acid, pH 4.5 for 1 hour at 37°C. The enzymatic reaction was then terminated by adding 0.1 M glycine buffer, pH 10.7. As a positive control, cells were lysed with 0.2% Triton X-100 to quantify the total β-hex content. The β-hex content was quantified by measuring fluorescence at ex360/em452 nm. For the antigen-dependent approach, human mast cells were incubated with serum pools from donors with milk allergy (n = 10) and donors tolerant of milk (n = 10), followed by incubation with apoBLG or holoBLG (5 nM). Degranulation was assessed by measurement of released ß-hex in the supernatant and unreleased enzyme in the respective cell lysate. The presented results were calculated as percentage release of total ß-hex content, with a release from unstimulated controls being 0.041%, from positive controls with anti-human IgE being 35% and with ionomycin being 94%.

Statistical analyses

Mouse groups and cellular studies were compared by performing ANOVA following the Tukey multiple comparisons test or using mixed effects analysis following the Sidak multiple comparisons test when some data points were missing. To compare the effects of different treatments on primary cells or binding of patient sera, we applied the Wilcoxon matched-pairs signed test when comparing 2 groups and repeated measures 1-way ANOVA following Tukey's multiple comparisons test when comparing more than 3 groups. All tests were 2 sided, and the results were considered significant when P was less than .05.

RESULTS
Quercetin-iron, but not ferrioxamine complexes, are bound by BLG

Quercetin, with a complex stability constant log β of 44.2 at pH 7.4,[31,59] binds strongly to ferric iron at physiologic pH. Importantly, BLG bound very strongly to FeQ2 complexes (Fig 1, *A*), with calculated affinities in the nM range (Fig 1, *B*), but not to non–catechol-based siderophores such as ferrioxamine. Complex formation with iron led to concentration-dependent quenching of quercetin fluorescence (Fig 1, *C*) and induced a visible color change (Fig 1, *D*). In spectral analysis, addition of BLG led to a marked decrease in the absorption peak at 330 nm and seemed to "revert" the induced color change following FeQ2 complex formation (Fig 1, *D*).

These data confirmed that quercetin at physiologic pH is usually present in a complex with iron and that BLG can absorb these complexes.

HoloBLG prevents antibody formation and reduces splenocytic cytokine release *in vivo*

Subsequently, we assessed whether ligand loading with FeQ2 complex to BLG had biologic implications *in vivo* by intranasally applying apoBLG or holoBLG to BALB/c mice. Thus, in the mice, we applied 100-fold less than the equivalent human dose of, for instance, the BLG naturally contained in a 200-mL glass of milk. The respiratory nasal mucosal surfaces are chronically
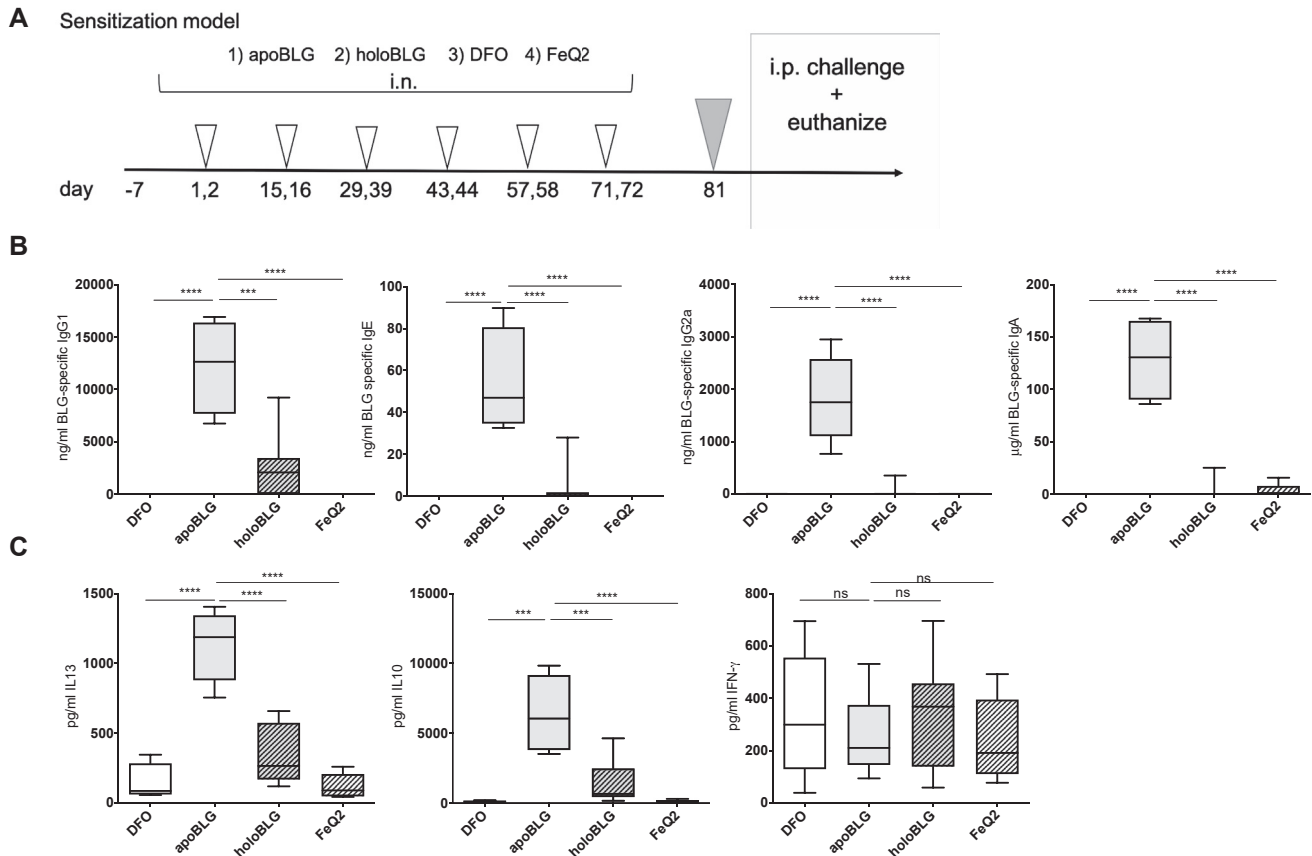
FIG 2. HoloBLG treatment prevents antibody formation and reduces splenocytic cytokine response. **A,** As depicted in the sensitization scheme, mice were intranasally sensitized 6 times at biweekly intervals with either apoBLG and equimolar concentrations of deferoxamine in the apoBLG group or apoBLG in combination with FeQ2 complexes, representing the holoBLG group, or sham-treated with FeQ2 complexes alone or deferoxamine (DFO) alone. Subsequently, the mice were challenged with BLG intraperitoneally, and allergic response was monitored before they were humanely killed. **B,** BLG-specific IgG1, IgE, IgG2a, and IgA-levels in serum. **C,** Splenocytic cytokine response of mice intranasally treated with DFO (n = 5), FeQ2 complex (n = 5), apoBLG (n = 5), and holoBLG (n = 5). Representative data from 3 independent experiments are shown. Groups were compared by using ANOVA following the Tukey multiple comparisons test. Data are represented as means ± SEMs. ***$P < .001$; ****$P < .0001$.

exposed not only to a myriad of antigens and commensal bacteria but also to iron. We needed to ensure that these local factors would not interfere with the apoBLG protocol so that during the sensitization process the calyx of apoBLG would remain empty. Therefore, for the intranasal apoBLG treatment, an equimolar concentration of the iron chelator deferoxamine,[60] a chemical approved by the US Food and Drug Administration for treating iron overload, was added to BLG to guarantee its apo form following mucosal application; a second group of mice were treated with "prefilled" holoBLG, and the control groups were sham-treated with deferoxamine or FeQ2 complex alone.

After 6 nasal applications (Fig 2, A) in the absence of any added adjuvants, only mice treated with the apo form of BLG had significantly elevated serum levels of BLG-specific IgG1, IgE, IgG2a, and IgA antibodies, whereas nasal exposure of mice to holoBLG prevented production of all BLG-specific immunoglobulin classes (Fig 2, B). In fact, the levels of antibodies in mice sensitized with holoBLG did not differ statistically from the levels in the control groups treated with deferoxamine or FeQ2 complex alone.

In accordance with the failure to produce BLG-specific antibodies in the holoBLG-treated mice, their splenocytes stimulated with BLG secreted significantly lower levels of T_H2 cell–associated and regulatory cytokines (Fig 2, C), showed significantly less proliferation and had significantly more Treg cells than did mice treated with apoBLG (Fig 3, A and B).

In line with the observed suppressed immunologic profile, allergen challenge led to systemic anaphylaxis only in the apoBLG-treated mice, whereas mice treated with the ligand-loaded holoBLG were protected from body temperature drop, physical impairment, and anaphylaxis symptoms (Fig 3, C).

As such, transport of FeQ2 ligands by BLG prevented specific immune responses that could lead to allergic symptoms or anaphylaxis.

The ligand quercetin provides an anti-inflammatory stimulus by activating the AhR *in vitro* and *in vivo*

As the sole difference between the BLG treatment protocols was the addition of ligands, we investigated the underlying molecular mechanisms for the quercetin-iron cargo of BLG.
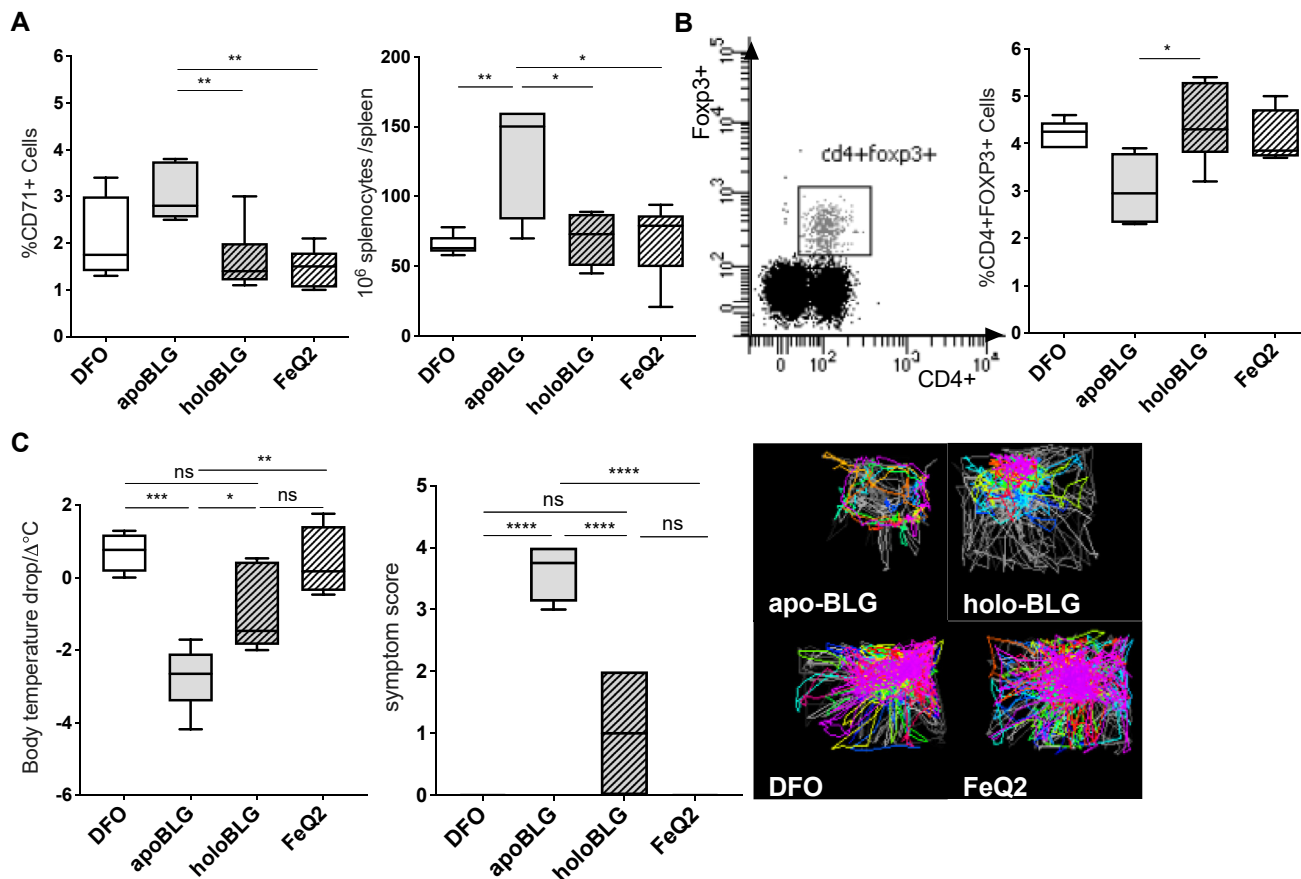
FIG 3. HoloBLG treatment prevents lymphocyte proliferation, promotes regulatory T cells, and protects against allergic reactions. Splenocytes of the groups treated with deferoxamine, apoBLG, holoBLG, or FeQ2 complex were analyzed for CD71 expression and total numbers of splenocytes per spleen (**A**) or for CD4 and Foxp3 coexpression (**B**). **C,** Body temperature drop, symptom score, and representative images of body temperature (*blue to red indicates low to high temperature*) and movements (*lines*) recorded by the imaging cage after systemic challenge with BLG in the different treated groups. Representative data from 3 independent experiments are shown. Groups were compared by 1-way ANOVA following the Tukey multiple comparisons test. Data are represented as means ± SEMs. *$P < .05$; **$P < .01$; ***$P < .001$; ****$P < .0001$.

Among receptor candidates, activation of the cytoplasmic promiscuous AhR has been described as mediating anti-inflammatory feedback mechanisms,[61] promoting Treg cells,[57,62,63] and suppressing T_H2 skewing[64,65] and antigen presentation.[66] AhR interacts with a plethora of exogenous ligands such as acrolein,[57] and importantly also with plant flavonoids such as quercetin,[67] emphasizing the participation of environmental or nutritional factors in immune regulation. Using reporter cells, we were able to demonstrate quercetin-dependent activation of the AhR pathway (Fig 4, *A*), which was significantly enhanced following the addition of BLG, implying synergy with directed targeting to the BLG receptors (Fig 4, *B*). Iron import is tightly regulated and requires active transport. As such, formation of iron complexes inhibited quercetin transport and consequently quercetin-dependent AhR-activation, which could (to a certain extent) be restored by addition of BLG. In line with the *in vitro* data, prominent expression of CYP1A1, a transcription factor downstream of AhR, was present in the lungs of holoBLG-treated mice compared with in the lungs of mice treated with apoBLG or controls (Fig 4, *C* and *D*). Hence, BLG is capable of transporting its cargo to cells and releasing it into them, leading

to AhR activation that contributes to the observed immune resilience.

Transport of FeQ2 complexes increases intracellular iron in monocytes and leads to impaired antigen presentation

The cargo of BLG also included the essential trace element iron. The iron status *per se* is critical for the activation status of antigen-presenting cells (in particular, that of macrophages), with a decrease resulting in immune activation, whereas an increase of "complexed iron" would lead to immunosuppression.[68-73] This is in contrast to "free" noncomplexed, non–protein-bound iron, which leads to the formation of reactive oxygen species. As depicted in Fig 5 and Fig E1 (in this article's Online Repository at www.jacionline.org), in primary human monocytic cells, incubation with the ligand-loaded holo form resulted in an increase of intracellular iron, as measured by the quenching of the calcein signal and compared with the signal of monocytic cells incubated together with apoBLG. Interestingly, this phenomenon was restricted to the monocytic CD14^{+}
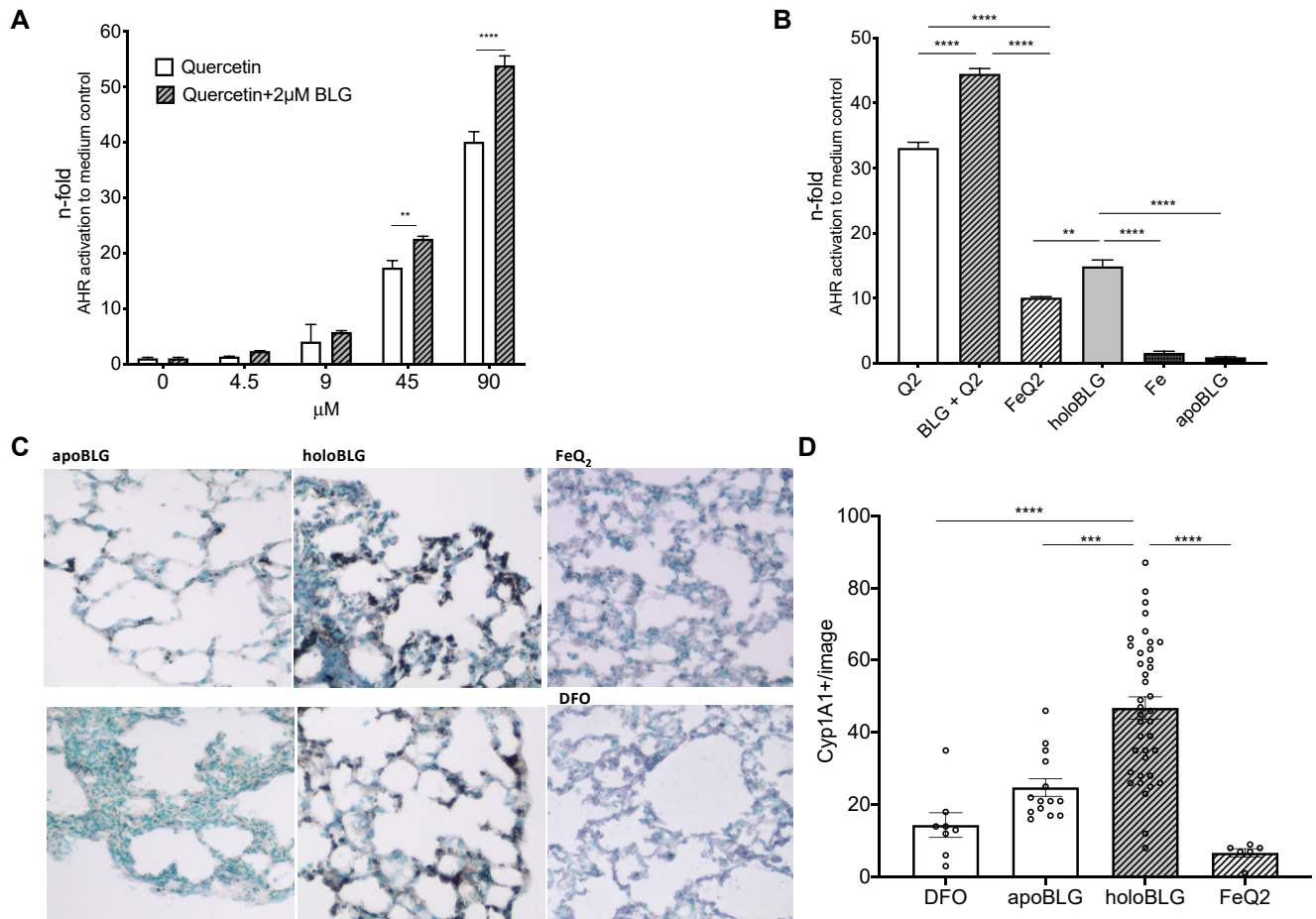
FIG 4. BLG promotes quercetin-dependent AhR activation. AZ-AHR cells were treated with increasing concentrations of quercetin alone (0, 4.5, 9, 45, or 90 μM) or quercetin and 2 μM BLG (**A**) or with 90 μM quercetin in combination with 45 μM iron and/or 2 μM BLG (**B**) for 18 hours before luciferase activity was measured in the supernatant. Representative data from 3 independent experiments normalized to medium alone are shown. **C**, Representative regions of lung sections stained for Cyp1A1. **D**, Quantification of Cyp1A1 expression per image in the differently treated mice. Concentration-dependent activation of AhR was compared by using mixed-effects analysis following the Sidak multiple comparisons test. Differences between quercetin activation in the presence or absence of iron and BLG and Cyp1a1 expression were tested by 1-way ANOVA following the Tukey multiple comparisons test. Data are represented as means ± SDs; **P < .01; ***P < .001; ****P < .0001.

compartment (Fig 5, *A*) and did not extend to CD3$^+$ T cells, in which no increase in the intracellular iron levels and no changes in the relative CD3$^+$ numbers were observed (Fig 5, *B* and see Fig E2 in this article's Online Repository at www.jacionline.org). HoloBLG treatment did not result in increased cell death in the general cellular population (see Fig E3) but did affect, as previously reported,[23] the relative abundance of CD3$^+$CD4$^+$ subsets (see Fig E2) and the CD14$^+$ population (see Fig E1). Further analyses of the CD14$^+$ population revealed that holoBLG treatment decreased HLADR expression, resulting in lower relative numbers of CD14$^+$HLADR$^+$CD86$^+$ cells (Fig 5, *C* and see Fig E1). In its apo form, BLG was a potent immune stimulator and led to secretion of T$_H$2-associated cytokines even in iron-deficient conditions (Fig 5, *D* and *E*). In contrast, uptake of BLG with ligands led to an increase of intracellular iron in monocytes and impaired antigen presentation by downregulating MHC class 2 and costimulatory molecules, thereby preventing immune activation and cytokine secretion.

Ligand binding masks B- and T-cell epitopes of BLG affecting IgE binding and mast cell degranulation

As antigen presentation was clearly impaired, we further analyzed the possible direct impact of FeQ2 ligands on BLG epitope regions. We compared the ligand binding site with known IgE and T-cell epitopes of BLG. For BLG, 2 experimentally deduced dominant IgE epitope regions were reported at residues K75 to D85 in a loop and E127 to P144 at the site of the α-helix,[26] with "weaker" IgE epitopes described at segments defined by residues L31 to P48, K47 to K60, and L57 to I78. As depicted in Fig 6, *A*, the ligand binding site was in close proximity to the IgE epitope 1, which was described as being relevant in subjects with persistent milk allergy[74] but did not affect epitope 2, which is located at the opposite site of epitope 1 on the α-helix. To determine whether ligand binding had any biologic consequence in humans, we determined IgE binding to BLG, with or without ligands, in milk-sensitized children who reacted
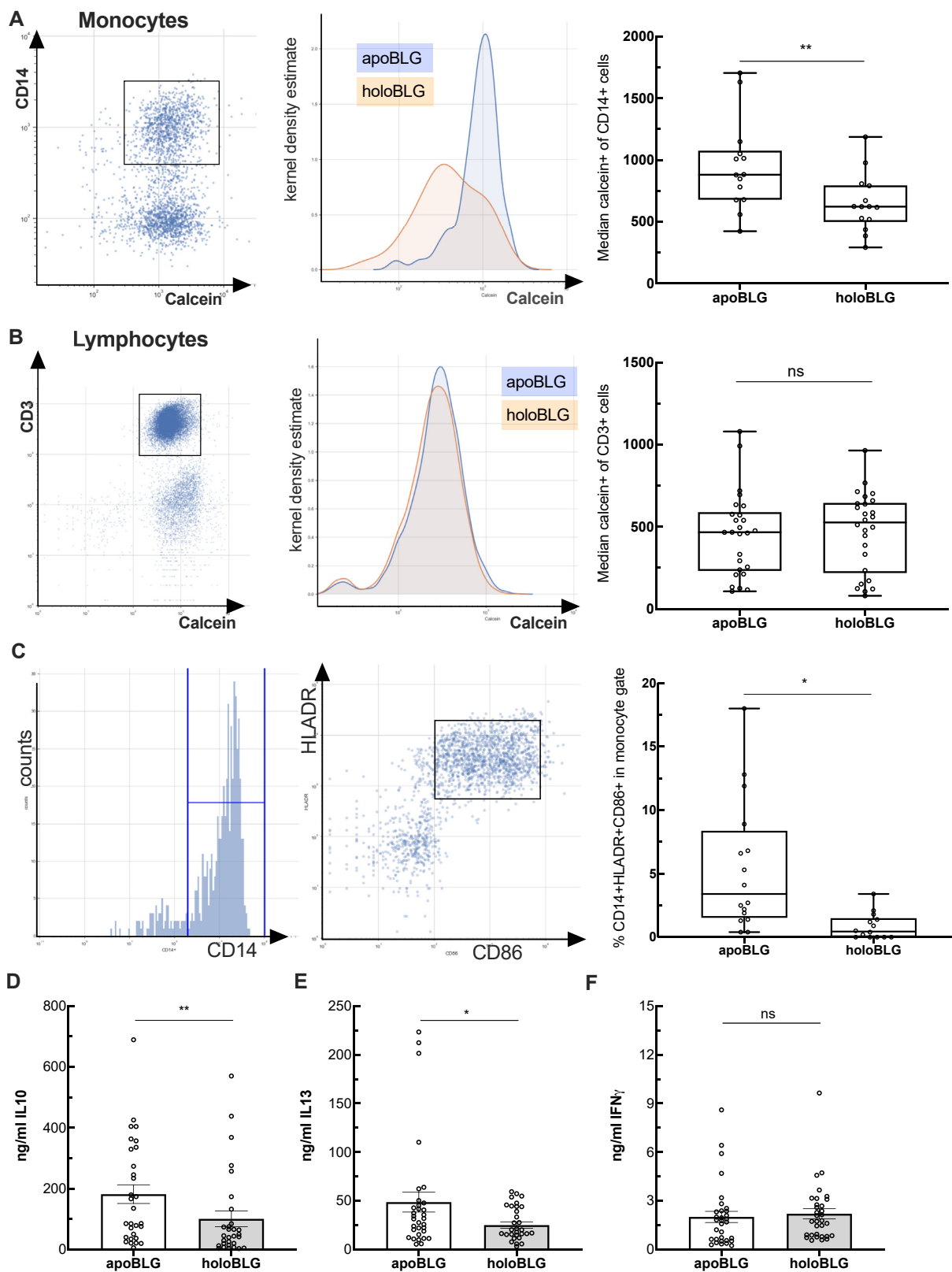
FIG 5. HoloBLG increases intracellular iron in monocytic cells but not in T cells. PBMCs isolated by density gradient (n = 16) were incubated overnight in iron-free media and in the presence or absence of apoBLG (*blue curve*) or holoBLG (*orange curve*) before analysis for an increase in intracellular iron levels by means of quenching of the calcein signal. Summary of the calcein signal in the monocytic gate (**A**) and CD3^{+} cells (**B**). **C,** HLADR^{+}CD86^{+} expression of CD14^{+} cells. IL-10 (**D**), IL-13 (**E**), and IFN-γ (**F**) levels after 18 hours of incubation in iron-free media. Data from 5 independently performed experiments with a total of 16 subjects are shown. Groups were compared by using the Wilcoxon matched-pairs signed test. Data are represented as means ± SEMs. *P < .05; **P < .01.
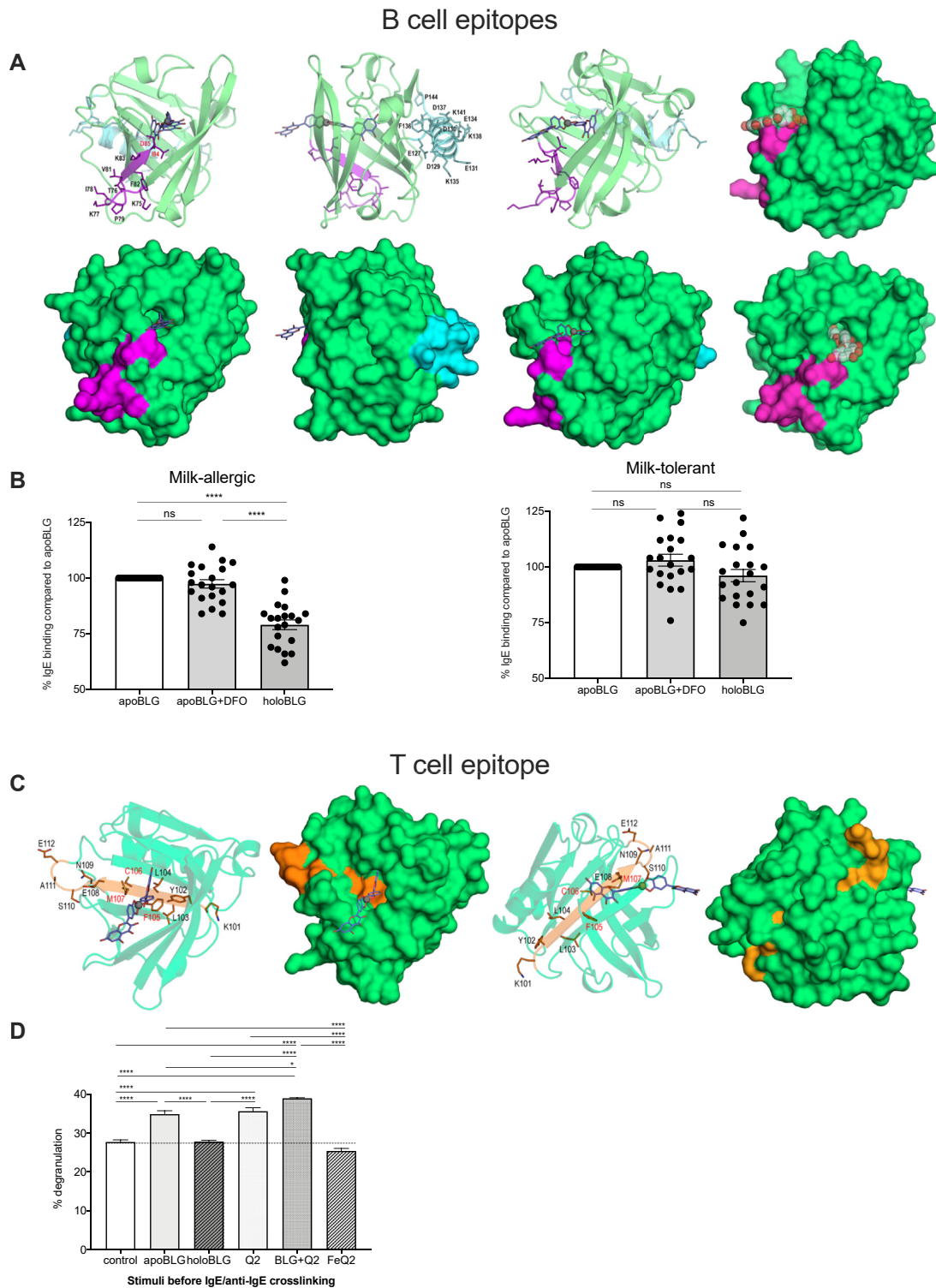
FIG 6. Ligand binding masks B-cell and T-cell epitopes of BLG affecting IgE binding and antigen-independent mast cell degranulation. **A,** Localization in the structure (*cartoons and sticks in upper row*) and on the surface (*lower row*) of 2 IgE-binding epitopes in BLG: epitope 1 (residues 75-85) is colored magenta, and epitope 2 (residues 127-144) is colored cyan. Labels in red indicate residues within a distance of 4 Å from the FeQ2 ligand (*shown as sticks with carbons in deep blue in the 3 cases*). In the right column, ligands are depicted as partially transparent spheres and sticks underneath. **B,** IgE binding to BLG alone or in combination with deferoxamine and FeQ2 complex in children allergic to milk (n = 20) and children tolerant of milk (n = 20), respectively. **C,** The dominant T-cell epitope defined by residues Y102 to E112 are marked in orange in 2 views of the BLG- FeQ2 complex. Surface images correspond to the orientation shown in the cartoon images. **D,** Antigen-independent impact of BLG in combination with the ligands on human mast cell degranulation. Groups were compared for (**B**) by repeated measures 1-way ANOVA following the Tukey multiple comparisons test and for (**D**) by 1-way ANOVA following the Tukey multiple comparisons test. Data are represented as means ± SEMs. *P < .05; ****P <.0001.

positively (n = 20) and negatively (n = 20) to oral cow's milk challenge, termed *allergic to milk* and *tolerant of milk*, respectively (Fig 6, *B* and see the patient characteristics in Table E1 in this article's Online Repository at www.jaclonline. org). Indeed, the subjects with milk allergy had reduced IgE binding to the holo form of BLG, loaded with FeQ2 complexes, compared with apoBLG or when an irrelevant chelator such as deferoxamine was used. Importantly, the IgE binding of children tolerant of milk was not affected by the ligands of BLG, emphasizing that the IgE of children tolerant of milk recognizes different epitopes that are not in close proximity to the ligand binding site. It also underscores the fact that the IgE in children allergic to milk is formed under conditions in which BLG is devoid of ligands and thus fulfills the requirements for allergenicity.

Next, we addressed whether ligand binding also affected the immunodominant T-cell epitope for BLG, located at residues 97 to 117, with the most important core residues Y102 to E112 (YLLFCMENSAE).[26,75,76]

As clearly shown in Fig 6, *C*, ligand binding colocalized in particular with the T-cell epitope residues F105, C106, and M107. Antigen stability is crucial for antigen processing and can determine the sensitizing potential of allergens by altering epitope-specific T-cell activation as described for the major birch pollen allergen *Betula verrucosa* 1 in 2 studies.[77,78] Endolysosomal enzymes such as cathepsin S process antigens to peptides for presentation. Interestingly, 2 of its predicted cleavage sites are located within the dominant T-cell epitope at BLGp99-105 and BLGp109-115,[26] suggesting that here also, ligands masking the position F105 prevent proper endolysosomal processing and antigen processing.

The colocalization strongly suggests that ligand binding impaired the T-cell–stimulatory capacity of the holoBLG in our *in vivo* murine model as well as in human PBMCs *in vitro* (Figs 3, *A* and 5, *D*, respectively).

As binding of FeQ2 complex to BLG masked IgE and T-cell epitopes and affected antigen presentation, we also addressed whether the ligands alone had an impact in the effector phase by using primary human mast cells in an antigen-independent approach (Fig 6, *D*). Here, IgE-sensitized mast cells were preincubated with BLG, quercetin, or FeQ2 complexes, alone and in combinations thereof, before being crosslinked via anti-IgE. Also in this setting, only apoBLG and quercetin, which are able to sequester iron, promoted mast cell degranulation. In contrast, holoBLG did not further sensitize these cells, suggesting a role for iron in this resilience state (Fig 6, *D*). This is in line with the literature showing that depending on the degree of iron saturation, lactoferrin and transferrin can inhibit the degranulation capacity of cells *in vitro* and *in vivo*.[79-81]

DISCUSSION

Here we have revealed a previously unrecognized function of the lipocalin BLG, the major whey compound of milk, to provide immune tolerance when loaded with FeQ2 complex. Our data suggest that proper loading prevents the antigenicity of the cow's milk allergen itself, on the one hand, by masking important immune epitopes, and on the other hand, by shuttling ligands to immune cells that downtune their antigen presentation skills. HoloBLG shuttled complexed iron into antigen-presenting cells but not into lymphocytes, and it reduced the readiness of mast cells to degranulate.

Our data suggest that the nasal mucosa may represent a natural route for tolerance induction to airborne BLG from cattle farms, explaining the allergy-protective effect of farm living. We propose that BLG could be exploited for mucosal tolerance induction in preventive or therapeutic settings.

Molecular studies also showed that the tolerogenic aryl hydrocarbon receptor pathway was activated. AhR expression levels vary in immune cells, with high expression levels found in monocytes,[82] dendritic cells, macrophages,[83] and B cells.[84,85] Within the T-cell compartments, T_H17 cells, and to a lesser extent Treg cells, express AhR.[86] Importantly AhR activation has been reported to reduce inflammation,[87,88] abrogate T_H2 cell differentiation, downregulate FcεRI expression on antigen-presenting cells,[61] and promote Treg cells.[89,90] In line with the literature, we have shown concentration-dependent AhR activation by quercetin, which was significantly enhanced by the addition of BLG *in vitro* in a reporter cell system. Moreover, Cyp1A1 expression was significantly upregulated in the lungs of holoBLG-treated mice, which is associated with protection to allergic sensitization, a sustainment of Treg cells, and reduced clinical immediate-type reactivity. As we were not able to detect Cyp1A1 expression in the controls, in which only FeQ2 complexes were applied without BLG, we propose that BLG is needed for effective ligand transport and activation of the AhR pathway *in vivo*.

We observed a general nonresponsiveness when applying BLG with its ligands *in vivo* in terms of humoral and cellular responses, with reduced release of cytokines including immune-suppressive cytokine IL-10. This resilience to immune activation resembles observed findings that subjects who do not yet have an allergy neither possess more Treg cells nor secrete more IL-10 than do subjects with an allergy.[91] This is in contrast to the finding that subjects who formerly had an allergy and now have secondarily acquired tolerance clearly show increased levels of Treg cells and IL-10.[92]

We also identified iron as an underappreciated contributor to immune tolerance. Indeed, iron deficiency favors a T_H2 response[93-95] and allergy,[96-98] whereas too much iron leads to immunosuppression,[99] partly by increasing the ratio of Treg cells in relation to effector T cells.[100,101]

An increase in intracellular iron has been linked to impaired antigen presentation and is associated with a suppressive phenotype in macrophages *in vitro* and *in vivo*.[69] In contrast, reduced cellular iron content in macrophages enhances the generation of proinflammatory cytokines.[71] Similarly, increased iron levels negatively affect $CD4^+$ cell counts,[102] and to a lesser extent $CD8^+$ cells.[72] Accordingly, our *in vitro* evidence suggests that holoBLG is primarily taken up by antigen-presenting cells rather than by T cells. Additionally, epitope masking, a simultaneous increase of intracellular iron, and initiation of the AhR cascade prevents effective antigen presentation.[103] Our data also show an impact of iron in the effector phase of allergy, where it directly acts on mast cells in an antigen-unspecific manner and lowers mediator release. In contrast, iron-free apoBLG as well as quercetin, as an iron chelator, alone or in combination with BLG, increased the degranulatory ability of these mast cells. Similarly, studies have shown that histamine release from mast cells can be inhibited *in vitro*[79] and *in vivo*[79] depending on their degree of iron saturation by iron-laden lactoferrin and transferrin.[79,81]

The loading state of BLG could indeed be the nexus between the allergenic or tolerogenic state of this major whey compound

and likely expand to other ligands such as retinoic acid that mask the immunodominant T-cell epitope of BLG.[26]

This finding is also hinted at by the reduced IgE recognition of the loaded BLG molecule by IgE of children allergic to milk, implying that children with milk allergy at a certain time point generated IgE against the "naked" epitopes of an apoBLG form. It is also in contrast to children sensitized to but tolerating milk, who did not discriminate between the filled or empty proteins, which may reflect IgE binding to minor BLG epitopes not affected by ligand binding.

The immune system has evolved to survey and respond to environmental stimuli. In this regard, BLG as an innate defense protein seems to hunt for ligands and nutrients and in humans confer protection by calming immune cells, via its ability to transport ligands to our immune cells.

The study may also have implications for understanding the allergy- and asthma-protective effects of farm milk and living in a farm environment, as the holoBLG loaded with its ligands might preferentially occur in nonprocessed, nondefatted milk.

Indeed, binding of polyphenols (catechins,[104,105] quercetin,[36,106] luteolin,[107] rutin,[36] etc) has been reported to increase the antioxidant activity of BLG[105,108,109] and lead to enhanced intestinal uptake.[110] In contrast, BLG depletion reduces the antioxidant activities of milk by 50%, whereas purified BLG is considered only a mild antioxidant.[111] Studies have also shown that the ability of BLG to bind to ligands such as retinol and palmitic acid is lost following heating,[112] just as the antioxidant activity in milk is reduced after heating,[111,113] while its antigenicity is increased at the same time.[26,112]

Collectively, we have discovered a previously unrecognized role of the major milk protein BLG to transport ligands to immune cells, thereby providing an immune-regulatory effect resulting in resilience to immune activation and protection against allergic sensitization and symptoms. Our findings propose that spiking BLG with natural ligands such as quercetin or retinoic acid may pave the path toward a new generation of prophylactic or therapeutic approaches against the allergy epidemic.

Key messages

- **Ligands of BLG, such as FeQ2 complexes, are decisive in preventing allergic sensitization *in vitro* and *in vivo*.**

- **Ligand binding masks major IgE and T-cell epitopes of BLG with IgE of patients with milk allergy showing reduced binding to the ligand-loaded holo form of BLG.**

- **Delivery of FeQ2 complexes by BLG to antigen-presenting cells increased intracellular iron levels while decreasing their antigen presentation capacities.**

- **The released complexes activated the aryl hydrocarbon receptor pathway, sustaining the numbers of Treg cells *in vivo*.**

- **Immune reactions to the empty, unloaded form of BLG were in significant contrast to the observations with the loaded holo form and resulted in specific allergy.**

REFERENCES

1. Jordakieva G, Kundi M, Untersmayr E, Pali-Scholl I, Reichardt B, Jensen-Jarolim E. Country-wide medical records infer increased allergy risk of gastric acid inhibition. Nat Commun 2019;10:3298.
2. Stein MM, Hrusch CL, Gozdz J, Igartua C, Pivniouk V, Murray SE, et al. Innate immunity and asthma risk in amish and hutterite farm children. N Engl J Med 2016;375:411-21.
3. Ege MJ, Mayer M, Normand AC, Genuneit J, Cookson WO, Braun-Fahrlander C, et al. Exposure to environmental microorganisms and childhood asthma. N Engl J Med 2011;364:701-9.
4. Waser M, Michels KB, Bieli C, Floistrup H, Pershagen G, von Mutius E, et al. Inverse association of farm milk consumption with asthma and allergy in rural and suburban populations across Europe. Clin Exp Allergy 2007;37: 661-70.
5. Brick T, Schober Y, Bocking C, Pekkanen J, Genuneit J, Loss G, et al. Omega-3 fatty acids contribute to the asthma-protective effect of unprocessed cow's milk. J Allergy Clin Immunol 2016;137:1699-706.e13.
6. Jonsson K, Barman M, Moberg S, Sjoberg A, Brekke HK, Hesselmar B, et al. Fat intake and breast milk fatty acid composition in farming and nonfarming women and allergy development in the offspring. Pediatr Res 2016;79:114-23.
7. Loss G, Apprich S, Waser M, Kneifel W, Genuneit J, Buchele G, et al. The protective effect of farm milk consumption on childhood asthma and atopy: the GABRIELA study. J Allergy Clin Immunol 2011;128:766-3.e4.
8. Abbring S, Kusche D, Roos TC, Diks MAP, Hols G, Garssen J, et al. Milk processing increases the allergenicity of cow's milk-preclinical evidence supported by a human proof-of-concept provocation pilot. Clin Exp Allergy 2019;49: 1013-25.
9. Lam HY, van Hoffen E, Michelsen A, Guikers K, van der Tas CH, Bruijnzeel-Koomen CA, et al. Cow's milk allergy in adults is rare but severe: both casein and whey proteins are involved. Clin Exp Allergy 2008;38:995-1002.
10. Kaczmarski M, Wasilewska J, Cudowska B, Semeniuk J, Klukowski M, Matuszewska E. The natural history of cow's milk allergy in north-eastern Poland. Adv Med Sci 2013;58:22-30.
11. Jensen-Jarolim E, Pacios LF, Bianchini R, Hofstetter G, Roth-Walter F. Structural similarities of human and mammalian lipocalins, and their function in innate immunity and allergy. Allergy 2016;71:286-94.
12. Roth-Walter F, Berin MC, Arnaboldi P, Escalante CR, Dahan S, Rauch J, et al. Pasteurization of milk proteins promotes allergic sensitization by enhancing uptake through Peyer's patches. Allergy 2008;63:882-90.
13. Fluckinger M, Merschak P, Hermann M, Haertle T, Redl B. Lipocalin-interacting-membrane-receptor (LIMR) mediates cellular internalization of beta-lactoglobulin. Biochim Biophys Acta 2008;1778:342-7.
14. Mansouri A, Gueant JL, Capiaumont J, Pelosi P, Nabet P, Haertle T. Plasma membrane receptor for beta-lactoglobulin and retinol-binding protein in murine hybridomas. Biofactors 1998;7:287-98.
15. Flower DR. Beyond the superfamily: the lipocalin receptors. Biochim Biophys Acta 2000;1482:327-36.
16. Hesselink RW, Findlay JB. Expression, characterization and ligand specificity of lipocalin-1 interacting membrane receptor (LIMR). Mol Membr Biol 2013;30: 327-37.
17. Devireddy LR, Gazin C, Zhu X, Green MR. A cell-surface receptor for lipocalin 24p3 selectively mediates apoptosis and iron uptake. Cell 2005;123:1293-305.
18. Roth-Walter F, Schmutz R, Mothes-Luksch N, Lemell P, Zieglmayer P, Zieglmayer R, et al. Clinical efficacy of sublingual immunotherapy is associated with restoration of steady-state serum lipocalin 2 after SLIT: a pilot study. World Allergy Organ J 2018;11:21.
19. Wojnar P, Lechner M, Redl B. Antisense down-regulation of lipocalin-interacting membrane receptor expression inhibits cellular internalization of lipocalin-1 in human NT2 cells. J Biol Chem 2003;278:16209-15.
20. Roth-Walter F, Jensen-Jarolim E, Gomez-Casado C, Diaz-Perales A, Pacios LF, Singer J. Method and means for diagnosing and treating allergy. EP 14150965.3, US 14/204,570 2014.
21. Bao G, Clifton M, Hoette TM, Mori K, Deng SX, Qiu A, et al. Iron traffics in circulation bound to a siderocalin (Ngal)-catechol complex. Nat Chem Biol 2010;6:602-9.
22. Fluckinger M, Haas H, Merschak P, Glasgow BJ, Redl B. Human tear lipocalin exhibits antimicrobial activity by scavenging microbial siderophores. Antimicrob Agents Chemother 2004;48:3367-72.
23. Roth-Walter F, Pacios LF, Gomez-Casado C, Hofstetter G, Roth GA, Singer J, et al. The major cow milk allergen Bos d 5 manipulates T-helper cells depending on its load with siderophore-bound iron. PLoS One 2014;9:e104803.
24. Chaneton L, Perez Saez JM, Bussmann LE. Antimicrobial activity of bovine beta-lactoglobulin against mastitis-causing bacteria. J Dairy Sci 2011;94:138-45.

25. Kanakis CD, Hasni I, Bourassa P, Tarantilis PA, Polissiou MG, Tajmir-Riahi HA. Milk beta-lactoglobulin complexes with tea polyphenols. Food Chem 2011;127: 1046-55.

26. Hufnagl K, Ghosh D, Wagner S, Fiocchi A, Dahdah L, Bianchini R, et al. Retinoic acid prevents immunogenicity of milk lipocalin Bos d 5 through binding to its immunodominant T-cell epitope. Sci Rep 2018;8:1598.

27. Stojadinovic M, Radosavljevic J, Ognjenovic J, Vesic J, Prodic I, Stanic-Vucinic D, et al. Binding affinity between dietary polyphenols and beta-lactoglobulin negatively correlates with the protein susceptibility to digestion and total antioxidant activity of complexes formed. Food Chem 2013;136:1263-71.

28. Rawel HM, Rohn S, Kroll J. Influence of a sugar moiety (rhamnosylglucoside) at 3-O position on the reactivity of quercetin with whey proteins. Int J Biol Macromol 2003;32:109-20.

29. Zhang L, Wang Y, Xu M, Hu X. Galloyl moieties enhance the binding of (-)-epigallocatechin-3-gallate to beta-lactoglobulin: a spectroscopic analysis. Food Chem 2017;237:39-45.

30. Keppler JK, Martin D, Garamus VM, Schwarz K. Differences in binding behavior of (-)-epigallocatechin gallate to beta-lactoglobulin heterodimers (AB) compared to homodimers (A) and (B). J Mol Recognit 2015;28:656-66.

31. Perron NR, Brumaghim JL. A review of the antioxidant mechanisms of polyphenol compounds related to iron binding. Cell Biochem Biophys 2009;53: 75-100.

32. Perron NR, Hodges JN, Jenkins M, Brumaghim JL. Predicting how polyphenol antioxidants prevent DNA damage by binding to iron. Inorg Chem 2008;47: 6153-61.

33. Cook GM, Loder C, Soballe B, Stafford GP, Membrillo-Hernandez J, Poole RK. A factor produced by Escherichia coli K-12 inhibits the growth of E. coli mutants defective in the cytochrome bd quinol oxidase complex: enterochelin rediscovered. Microbiology 1998;144(Pt 12):3297-308.

34. Khodr HH, Hider RC, Duhme-Klair AK. The iron-binding properties of aminochelin, the mono(catecholamide) siderophore of Azotobacter vinelandii. J Biol Inorg Chem 2002;7:891-6.

35. Roth-Walter F, Gomez-Casado C, Pacios LF, Mothes-Luksch N, Roth GA, Singer J, et al. Bet v 1 from birch pollen is a lipocalin-like protein acting as allergen only when devoid of iron by promoting Th2 lymphocytes. J Biol Chem 2014;289: 17416-21.

36. Mirpoor SF, Hosseini SMH, Nekoei AR. Efficient delivery of quercetin after binding to beta-lactoglobulin followed by formation soft-condensed core-shell nanostructures. Food Chem 2017;233:282-9.

37. Sahihi M, Heidari-Koholi Z, Bordbar A-K. The interaction of polyphenol flavonoids with β-lactoglobulin: molecular docking and molecular dynamics simulation studies. J Macromol Sci Part B 2012;51:2311-23.

38. Plundrich NJ, Bansode RR, Foegeding EA, Williams LL, Lila MA. Protein-bound Vaccinium fruit polyphenols decrease IgE binding to peanut allergens and RBL-2H3 mast cell degranulation in vitro. Food Funct 2017;8:1611-21.

39. Jacob T, von Loetzen CS, Reuter A, Lacher U, Schiller D, Schobert R, et al. Identification of a natural ligand of the hazel allergen Cor a 1. Sci Rep 2019;9:8714.

40. Garrido-Arandia M, Silva-Navas J, Ramirez-Castillejo C, Cubells-Baeza N, Gomez-Casado C, Barber D, et al. Characterisation of a flavonoid ligand of the fungal protein Alt a 1. Sci Rep 2016;6:33468.

41. Besle JM, Viala D, Martin B, Pradel P, Meunier B, Berdague JL, et al. Ultraviolet-absorbing compounds in milk are related to forage polyphenols. J Dairy Sci 2010; 93:2846-56.

42. Yu ES, Min HJ, An SY, Won HY, Hong JH, Hwang ES. Regulatory mechanisms of IL-2 and IFNgamma suppression by quercetin in T helper cells. Biochem Pharmacol 2008;76:70-8.

43. Tong Z, Wu X, Ovcharenko D, Zhu J, Chen CS, Kehrer JP. Neutrophil gelatinase-associated lipocalin as a survival factor. Biochem J 2005;391:441-8.

44. Kehrer JP. Lipocalin-2: pro- or anti-apoptotic? Cell Biol Toxicol 2010;26:83-9.

45. Shields-Cutler RR, Crowley JR, Hung CS, Stapleton AE, Aldrich CC, Marschall J, et al. Human urinary composition controls antibacterial activity of siderocalin. J Biol Chem 2015;290:15949-60.

46. Devireddy LR, Hart DO, Goetz DH, Green MR. A mammalian siderophore synthesized by an enzyme with a bacterial homolog involved in enterobactin production. Cell 2010;141:1006-17.

47. Grabenhenrich LB, Reich A, McBride D, Sprikkelman A, Roberts G, Grimshaw KEC, et al. Physician's appraisal vs documented signs and symptoms in the interpretation of food challenge tests: the EuroPrevall birth cohort. Pediatr Allergy Immunol 2018;29:58-65.

48. Kontopidis G, Holt C, Sawyer L. The ligand-binding site of bovine beta-lactoglobulin: evidence for a function? J Mol Biol 2002;318:1043-55.

49. Morris GM, Huey R, Lindstrom W, Sanner MF, Belew RK, Goodsell DS, et al. AutoDock4 and AutoDockTools4: automated docking with selective receptor flexibility. J Comput Chem 2009;30:2785-91.

50. Trott O, Olson AJ. AutoDock Vina: improving the speed and accuracy of docking with a new scoring function, efficient optimization, and multithreading. J Comput Chem 2010;31:455-61.

51. Carson M. Ribbons. Methods Enzymol 1997;277:493-505.

52. Pettersen EF, Goddard TD, Huang CC, Couch GS, Greenblatt DM, Meng EC, et al. UCSF Chimera–a visualization system for exploratory research and analysis. J Comput Chem 2004;25:1605-12.

53. Krissinel E, Henrick K. Inference of macromolecular assemblies from crystalline state. J Mol Biol 2007;372:774-97.

54. Moreland JL, Gramada A, Buzko OV, Zhang Q, Bourne PE. The Molecular Biology Toolkit (MBT): a modular platform for developing molecular visualization applications. BMC Bioinformatics 2005;6:21.

55. Manzano-Szalai K, Pali-Scholl I, Krishnamurthy D, Stremnitzer C, Flaschberger I, Jensen-Jarolim E. Anaphylaxis imaging: non-invasive measurement of surface body temperature and physical activity in small animals. PLoS One 2016;11: e0150819.

56. Novotna A, Pavek P, Dvorak Z. Novel stably transfected gene reporter human hepatoma cell line for assessment of aryl hydrocarbon receptor transcriptional activity: construction and characterization. Environ Sci Technol 2011;45: 10133-9.

57. Roth-Walter F, Bergmayr C, Meitz S, Buchleitner S, Stremnitzer C, Fazekas J, et al. Janus-faced acrolein prevents allergy but accelerates tumor growth by promoting immunoregulatory Foxp3+ cells: mouse model for passive respiratory exposure. Sci Rep 2017;7:45067.

58. Yu Y, Blokhuis BR, Garssen J, Redegeld FA. A transcriptomic insight into the impact of colon cancer cells on mast cells. Int J Mol Sci 2019;20.

59. El Hajji H, Nkhili E, Tomao V, Dangles O. Interactions of quercetin with iron and copper ions: complexation and autoxidation. Free Radic Res 2006;40:303-20.

60. Fine JM, Baillargeon AM, Renner DB, Hoerster NS, Tokarev J, Colton S, et al. Intranasal deferoxamine improves performance in radial arm water maze, stabilizes HIF-1alpha, and phosphorylates GSK3beta in P301L tau transgenic mice. Exp Brain Res 2012;219:381-90.

61. Koch S, Stroisch TJ, Vorac J, Herrmann N, Leib N, Schnautz S, et al. AhR mediates an anti-inflammatory feedback mechanism in human Langerhans cells involving FcepsilonRI and IDO. Allergy 2017;72:1686-93.

62. Gandhi R, Kumar D, Burns EJ, Nadeau M, Dake B, Laroni A, et al. Activation of the aryl hydrocarbon receptor induces human type 1 regulatory T cell-like and Foxp3(+) regulatory T cells. Nat Immunol 2010;11:846-53.

63. Quintana FJ, Basso AS, Iglesias AH, Korn T, Farez MF, Bettelli E, et al. Control of T(reg) and T(H)17 cell differentiation by the aryl hydrocarbon receptor. Nature 2008;453:65-71.

64. Xu T, Zhou Y, Qiu L, Do DC, Zhao Y, Cui Z, et al. Aryl hydrocarbon receptor protects lungs from cockroach allergen-induced inflammation by modulating mesenchymal stem cells. J Immunol 2015;195:5539-50.

65. Negishi T, Kato Y, Ooneda O, Mimura J, Takada T, Mochizuki H, et al. Effects of aryl hydrocarbon receptor signaling on the modulation of TH1/TH2 balance. J Immunol 2005;175:7348-56.

66. Aguilera-Montilla N, Chamorro S, Nieto C, Sanchez-Cabo F, Dopazo A, Fernandez-Salguero PM, et al. Aryl hydrocarbon receptor contributes to the MEK/ERK-dependent maintenance of the immature state of human dendritic cells. Blood 2013;121:e108-17.

67. Jin UH, Park H, Li X, Davidson LA, Allred C, Patil B, et al. Structure-dependent modulation of aryl hydrocarbon receptor-mediated activities by flavonoids. Toxicol Sci 2018;164:205-17.

68. Carrasco-Marin E, Alvarez-Dominguez C, Lopez-Mato P, Martinez-Palencia R, Leyva-Cobian F. Iron salts and iron-containing porphyrins block presentation of protein antigens by macrophages to MHC class II-restricted T cells. Cell Immunol 1996;171:173-85.

69. Agoro R, Taleb M, Quesniaux VFJ, Mura C. Cell iron status influences macrophage polarization. PLoS One 2018;13:e0196921.

70. Nairz M, Theurl I, Swirski FK, Weiss G. "Pumping iron"-how macrophages handle iron at the systemic, microenvironmental, and cellular levels. Pflugers Arch 2017;469:397-418.

71. Nairz M, Schroll A, Haschka D, Dichtl S, Sonnweber T, Theurl I, et al. Lipocalin-2 ensures host defense against Salmonella typhimurium by controlling macrophage iron homeostasis and immune response. Eur J Immunol 2015;45:3073-86.

72. Hagag AA, Elgamasy MA, Abd Elbar ES. Study of serum immunoglobulin levels and T lymphocyte subsets in children with beta thalassemia with iron overload in Egypt. Egypt J Immunol 2016;23:97-105.

73. Morikawa K, Oseko F, Morikawa S. A role for ferritin in hematopoiesis and the immune system. Leuk Lymphoma 1995;18:429-33.

74. Jarvinen KM, Beyer K, Vila L, Chatchatee P, Busse PJ, Sampson HA. B-cell epitopes as a screening instrument for persistent cow's milk allergy. J Allergy Clin Immunol 2002;110:293-7.

75. Inoue R, Matsushita S, Kaneko H, Shinoda S, Sakaguchi H, Nishimura Y, et al. Identification of beta-lactoglobulin-derived peptides and class II HLA molecules recognized by T cells from patients with milk allergy. Clin Exp Allergy 2001;31: 1126-34.

76. Sakaguchi H, Inoue R, Kaneko H, Watanabe M, Suzuki K, Kato Z, et al. Interaction among human leucocyte antigen-peptide-T cell receptor complexes in cow's milk allergy: the significance of human leucocyte antigen and T cell receptor-complementarity determining region 3 loops. Clin Exp Allergy 2002; 32:762-70.

77. Freier R, Dall E, Brandstetter H. Protease recognition sites in Bet v 1a are cryptic, explaining its slow processing relevant to its allergenicity. Sci Rep 2015;5:12707.

78. Machado Y, Freier R, Scheiblhofer S, Thalhamer T, Mayr M, Briza P, et al. Fold stability during endolysosomal acidification is a key factor for allergenicity and immunogenicity of the major birch pollen allergen. J Allergy Clin Immunol 2016;137:1525-34.

79. Theobald K, Gross-Weege W, Keymling J, Konig W. Inhibition of histamine release in vitro by a blocking factor from human serum: comparison with the iron binding proteins transferrin and lactoferrin. Agents Actions 1987;20:10-6.

80. Theobald K, Gross-Weege W, Keymling J, Konig W. Purification of serum proteins with inhibitory activity on the histamine release in vitro and/or in vivo. Int Arch Allergy Appl Immunol 1987;82:295-7.

81. Mecheri S, Peltre G, Lapeyre J, David B. Biological effect of transferrin on mast cell mediator release during the passive cutaneous anaphylaxis reaction: a possible inhibition mechanism involving iron. Ann Inst Pasteur Immunol 1987; 138:213-21.

82. Skazik-Voogt C, Kuhler K, Ott H, Czaja K, Zwadlo-Klarwasser G, Merk HF, et al. Myeloid human cell lines lack functional regulation of aryl hydrocarbon receptor-dependent phase I genes. ALTEX 2016;33:37-46.

83. Kreitinger JM, Beamer CA, Shepherd DM. Environmental immunology: lessons learned from exposure to a select panel of immunotoxicants. J Immunol 2016; 196:3217-25.

84. Vaidyanathan B, Chaudhry A, Yewdell WT, Angeletti D, Yen WF, Wheatley AK, et al. The aryl hydrocarbon receptor controls cell-fate decisions in B cells. J Exp Med 2017;214:197-208.

85. Villa M, Gialitakis M, Tolaini M, Ahlfors H, Henderson CJ, Wolf CR, et al. Aryl hydrocarbon receptor is required for optimal B-cell proliferation. EMBO J 2017; 36:116-28.

86. Esser C, Rannug A, Stockinger B. The aryl hydrocarbon receptor in immunity. Trends Immunol 2009;30:447-54.

87. Bessede A, Gargaro M, Pallotta MT, Matino D, Servillo G, Brunacci C, et al. Aryl hydrocarbon receptor control of a disease tolerance defence pathway. Nature 2014;511:184-90.

88. Goettel JA, Gandhi R, Kenison JE, Yeste A, Murugaiyan G, Sambanthamoorthy S, et al. AHR activation is protective against colitis driven by T cells in humanized mice. Cell Rep 2016;17:1318-29.

89. Ye J, Qiu J, Bostick JW, Ueda A, Schjerven H, Li S, et al. The aryl hydrocarbon receptor preferentially marks and promotes gut regulatory T cells. Cell Rep 2017; 21:2277-90.

90. Couroucli XI, Welty SE, Geske RS, Moorthy B. Regulation of pulmonary and hepatic cytochrome P4501A expression in the rat by hyperoxia: implications for hyperoxic lung injury. Mol Pharmacol 2002;61:507-15.

91. Bacher P, Heinrich F, Stervbo U, Nienen M, Vahldieck M, Iwert C, et al. Regulatory T cell specificity directs tolerance versus allergy against aeroantigens in humans. Cell 2016;167:1067-78.e16.

92. Qamar N, Fishbein AB, Erickson KA, Cai M, Szychlinski C, Bryce PJ, et al. Naturally occurring tolerance acquisition to foods in previously allergic children is characterized by antigen specificity and associated with increased subsets of regulatory T cells. Clin Exp Allergy 2015;45:1663-72.

93. Thorson JA, Smith KM, Gomez F, Naumann PW, Kemp JD. Role of iron in T cell activation: TH1 clones differ from TH2 clones in their sensitivity to inhibition of DNA synthesis caused by IgG Mabs against the transferrin receptor and the iron chelator deferoxamine. Cell Immunol 1991;134:126-37.

94. Jason J, Archibald LK, Nwanyanwu OC, Bell M, Jensen RJ, Gunter E, et al. The effects of iron deficiency on lymphocyte cytokine production and activation: preservation of hepatic iron but not at all cost. Clin Exp Immunol 2001;126:466-73.

95. Leung S, Holbrook A, King B, Lu HT, Evans V, Miyamoto N, et al. Differential inhibition of inducible T cell cytokine secretion by potent iron chelators. J Biomol Screen 2005;10:157-67.

96. Drury KE, Schaeffer M, Silverberg JI. Association between atopic disease and anemia in US children. JAMA Pediatr 2016;170:29-34.

97. Nwaru BI, Hayes H, Gambling L, Craig LC, Allan K, Prabhu N, et al. An exploratory study of the associations between maternal iron status in pregnancy and childhood wheeze and atopy. Br J Nutr 2014;112:2018-27.

98. Shaheen SO, Macdonald-Wallis C, Lawlor DA, Henderson AJ. Haemoglobin concentrations in pregnancy and respiratory and allergic outcomes in childhood: birth cohort study. Clin Exp Allergy 2017;47:1615-24.

99. Shaheen SO, Newson RB, Henderson AJ, Emmett PM, Sherriff A, Cooke M, et al. Umbilical cord trace elements and minerals and risk of early childhood wheezing and eczema. Eur Respir J 2004;24:292-7.

100. Zhang Q, Cui T, Chang Y, Zhang W, Li S, He Y, et al. HO-1 regulates the function of Treg: Association with the immune intolerance in vitiligo. J Cell Mol Med 2018;22:4335-43.

101. Chen J, Lu WY, Zhao MF, Cao XL, Jiang YY, Jin X, et al. Reactive oxygen species mediated T lymphocyte abnormalities in an iron-overloaded mouse model and iron-overloaded patients with myelodysplastic syndromes. Ann Hematol 2017;96:1085-95.

102. Cronin SJF, Seehus C, Weidinger A, Talbot S, Reissig S, Seifert M, et al. The metabolite BH4 controls T cell proliferation in autoimmunity and cancer. Nature 2018;563:564-8.

103. Yang D, Shui T, Miranda JW, Gilson DJ, Song Z, Chen J, et al. Mycobacterium leprae-infected macrophages preferentially primed regulatory T cell responses and was associated with lepromatous leprosy. PLoS Negl Trop Dis 2016;10: e0004335.

104. Chen W, Wang W, Ma X, Lv R, Balaso Watharkar R, Ding T, et al. Effect of pH-shifting treatment on structural and functional properties of whey protein isolate and its interaction with (-)-epigallocatechin-3-gallate. Food Chem 2019;274:234-41.

105. Tao F, Xiao C, Chen W, Zhang Y, Pan J, Jia Z. Covalent modification of beta-lactoglobulin by (-)-epigallocatechin-3-gallate results in a novel antioxidant molecule. Int J Biol Macromol 2019;126:1186-91.

106. Salvi A, Carrupt P, Tillement J, Testa B. Structural damage to proteins caused by free radicals: asessment, protection by antioxidants, and influence of protein binding. Biochem Pharmacol 2001;61:1237-42.

107. Li X, Lu Y, Deng R, Zheng T, Lv L. Chemical components from the haulm of Artemisia selengensis and the inhibitory effect on glycation of beta-lactoglobulin. Food Funct 2015;6:1841-6.

108. Zommara M, Toubo H, Sakono M, Imaizumi K. Prevention of peroxidative stress in rats fed on a low vitamin E-containing diet by supplementing with a fermented bovine milk whey preparation: effect of lactic acid and beta-lactoglobulin on the antiperoxidative action. Biosci Biotechnol Biochem 1998;62:710-7.

109. Bartfay WJ, Davis MT, Medves JM, Lugowski S. Milk whey protein decreases oxygen free radical production in a murine model of chronic iron-overload cardiomyopathy. Can J Cardiol 2003;19:1163-8.

110. Wang X, Ai T, Meng XL, Zhou J, Mao XY. In vitro iron absorption of alpha-lactalbumin hydrolysate-iron and beta-lactoglobulin hydrolysate-iron complexes. J Dairy Sci 2014;97:2559-66.

111. Liu HC, Chen WL, Mao SJ. Antioxidant nature of bovine milk beta-lactoglobulin. J Dairy Sci 2007;90:547-55.

112. Song CY, Chen WL, Yang MC, Huang JP, Mao SJ. Epitope mapping of a monoclonal antibody specific to bovine dry milk: involvement of residues 66-76 of strand D in thermal denatured beta-lactoglobulin. J Biol Chem 2005; 280:3574-82.

113. Kim YE, Kim JW, Cheon S, Nam MS, Kim KK. Alpha-casein and beta-lactoglobulin from cow milk exhibit antioxidant activity: a plausible link to antiaging effects. J Food Sci 2019;84:3083-90.
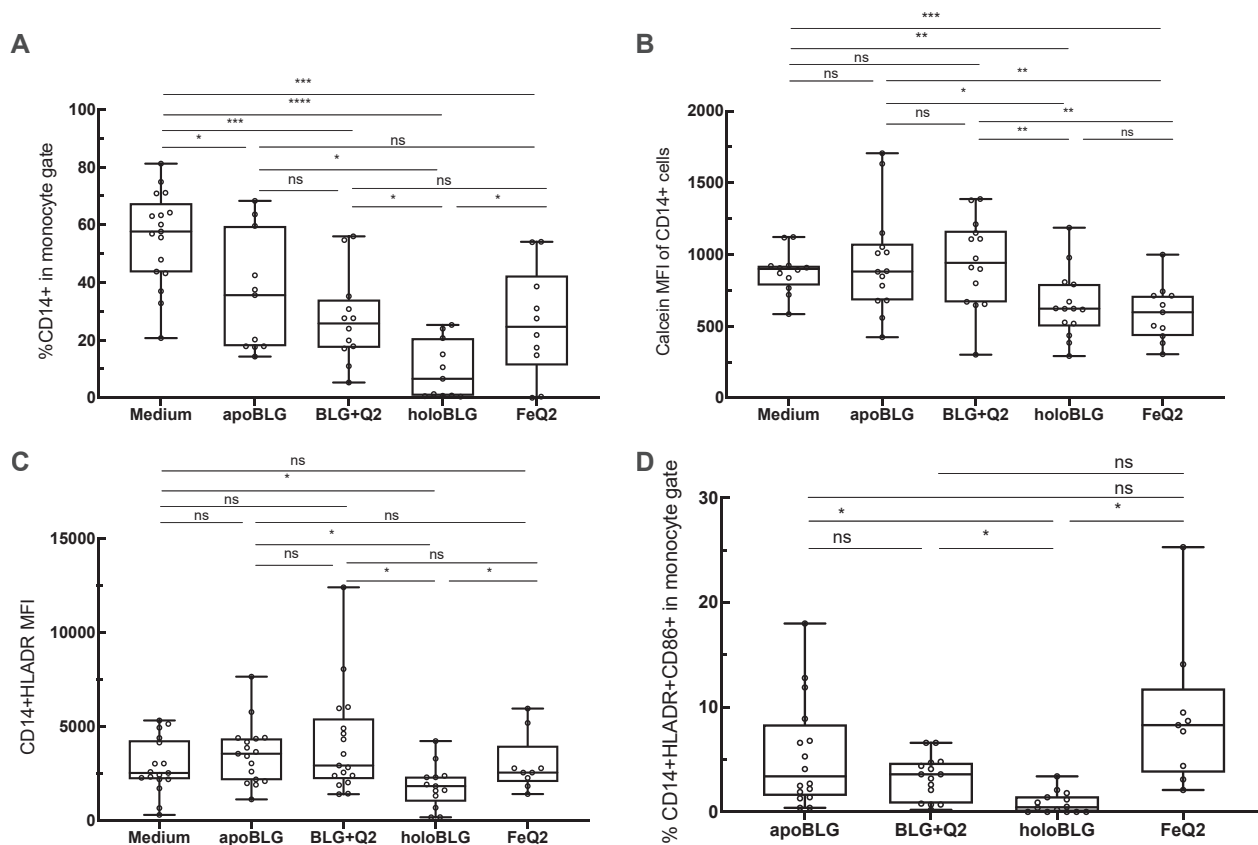
FIG E1. HoloBLG treatment increased intracellular iron in CD14$^+$ monocytic cells while decreasing HLADR expression and the relative CD14$^+$ cell population. Impact of stimulants on intracellular iron and cell populations. PBMCs were incubated overnight in iron-free media alone or with quercetin or FeQ2 in the presence or absence of BLG before analysis for CD14$^+$, HLADR, and monitoring intracellular iron levels by calcein staining. Relative numbers (**A**) and intracellular iron levels (**B**) of CD14$^+$ cells and MFI of HLADR (**C**) and CD86 (**D**) of CD14$^+$ cells. Groups were compared by repeated measures 1-way ANOVA following the Tukey multiple comparisons test. *P < .05; **P < .01; ***P < .001.

FIG E2. No significant differences in cell death in the gated cell population. PBMCs were incubated overnight in iron-free media alone or with quercetin or FeQ2 in the presence or absence of BLG. Cells were stained with calcein and gated to the lymphocytic and monocytic compartment. Calcein-negative cells within the gate were considered dead. Gating strategy (**A**), and absolute (**B**) and relative (**C**) numbers of calcein-negative cells within the gate. Groups were compared by repeated measures 1-way ANOVA following the Tukey multiple comparisons test, Data are represented as means ± SEMs.

FIG E3. HoloBLG treatment reduced intracellular iron and relative numbers of CD3$^+$CD4$^+$ cells. Impact of stimulants on intracellular iron and cell populations. PBMCs were incubated overnight in iron-free media alone or with quercetin or FeQ2 in the presence or absence of BLG before analysis for CD3$^+$CD4$^+$ cells and intracellular iron levels by means of quenching of the calcein signal. Relative numbers of CD3$^+$ cells (**A**) and CD3$^+$CD4$^+$ cells (**B**); intracellular iron levels in CD3$^+$ cells (**C**) and CD3$^+$CD4$^+$ cells (**D**). Groups were compared by repeated measures 1-way ANOVA following the Tukey multiple comparisons test. *P <.05; **P < .01; ***P <.001.

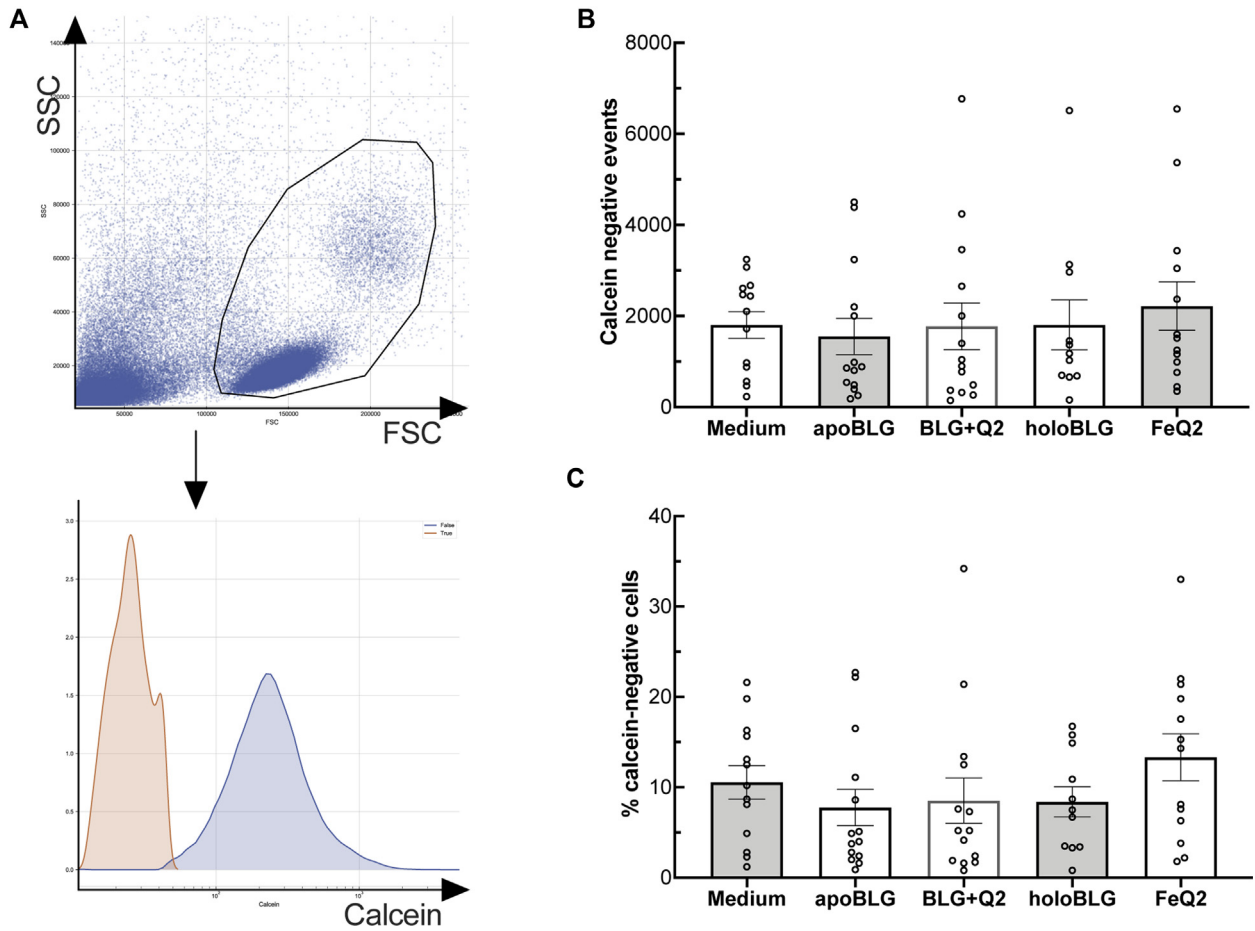**TABLE E1.** Characteristics of children allergic to milk and children tolerant of milk

Patient characteristic	Allergic to milk	Tolerant of milk	*P* value
n	20	20	ns
Age (mo), mean ± SD	71 ± 57	52 ± 30	.197
Sex (F/M)	7/13	5/15	
IgE total (kU/L), mean ± SD	867 ± 2718	235 ± 283	.334
IgE milk (kU/L), mean ± SD	29 ± 25	2.1 ± 6.9	.001

F, Female; *M*, male.